

**Investigation of Laser  $\mu$ -3D printed Triboelectric  
nanogenerator for energy harvesting**

**M.Tech. THESIS**

**By**

**AYUSH SINGH**



**Department of Mechanical Engineering**

**Indian Institute of Technology**

**Indore**

**MAY 2023**

**Dedicated to my  
Parents and Family**



# Indian Institute of Technology Indore

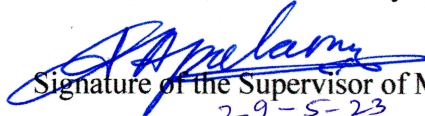
## CANDIDATE'S DECLARATION

I hereby certify that the work being presented in the thesis titled **Investigation of Laser  $\mu$ -3D printed Triboelectric nanogenerator for energy harvesting** in the partial fulfilments of the requirements for the award of the degree of **M.Tech. THESIS** and submitted in the **Department of Mechanical Engineering, Indian Institute of Technology, Indore** is an authentic record of my own work performed during the time period of April, 2022 to May, 2023 under the supervision of Prof. I. A Palani, Department of Mechanical Engineering, Indian Institute of Technology, Indore.

The matter presented in the thesis has not been submitted by me for the award of any other degree of this or any other institute.

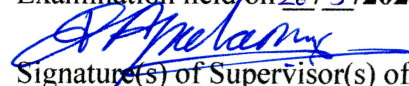
  
Signature of the student with date  
(Ayush Singh)

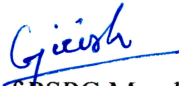
This is to certify that the above statement made by the candidate is correct to the best of my/our knowledge.

  
Signature of the Supervisor of M.Tech. thesis (with date)  
Prof. I.A. Palani

AYUSH SINGH has successfully given his/her M.Tech. Oral

Examination held on 26/5/2023.

  
Signature(s) of Supervisor(s) of  
M.Tech. thesis  
Date: 29/5/23

  
Signature of PSPC Member#1  
Date: 29/5/23

  
Signature of Head of Discipline with date:  
(Acting)

  
Signature of Convener  
DPGC  
Date: 29/05/2023  
  
Signature of PSPC Member#2  
Date:

## ACKNOWLEDGEMENTS

First, I would like to express my deepest gratitude and acknowledge my research guide **Prof. I. A. Palani**, Mechatronics and Instrumentation Lab, for his continuous guidance, patience, motivation, and enthusiasm. His valuable advice, constructive criticism, extensive discussions, and immense knowledge helped me to build a basic understanding of the subject and accomplish my thesis. His research methodology of developing practical application has been inspiring. During my time of association with him, I learnt a lot of things, both in life and career. He has tremendous multi-tasking and man management skills, which is something I would like to learn and carry with me in life. He has been a mentor who is always true to his position.

I would like to thank **Prof. Suhas Joshi**, Director, IIT Indore, **Dr. S. Dinakaran**, Head of Department, Mechanical Engineering, for supporting me with the sophisticated facilities to conduct my research. I would also like to thank PSPC members **Dr. Eswara Korimilli** and **Dr. Girish Verma** for giving their precious time for my assessment and for their valuable comments and suggestions towards enhancing my research work. My sincere thanks **Dr. Satyanarayana Patel**, DPGC convener for his sincere support.

I would like to thank **Department of Mechanical Engineering, IIT Indore** as well as **Department of MEMS, IIT Indore** for allowing access to the facility of various characterization techniques and providing a pleasant atmosphere for research. I would also like to acknowledge **HoD, Department of Mechanical Engineering, IIT Indore** for his constant support throughout the journey.

My Sincere appreciation to **Prof. Vipul Singh** Molecular and Nano Research Lab, Electrical Engineering Department, **Dr. Sunil Kumar**, Solid State Ionics Lab, MEMS Department, IIT Indore for their valuable support and fruitful discussion during the process. My appreciation also extends to **Opto- Mechatronics Group** for their

strong support and stimulating discussions. Also, I would like to admire my colleagues for their constant care and endorsement through this period. My sincere appreciation extends to my B.Tech inmates Piyush, Vijay, Kailash, for their help and support during my work. Mr. Mayank have constantly helped me with my work and my deepest gratitude goes to them as well. I would also like to acknowledge my school and college friends for being my constant support during my highs and lows.

Finally, I would like to express my deepest gratitude and respect to my parents for introducing me to this world and for being an ever-supportive rock in my life with their unflinching support.

I also acknowledge MHRD for their financial assistance to the research work carried out.

## ABSTRACT

3D printing or Additive manufacturing has gained its popularity due to its high innovations, process improvement and design freedom to many industries, including aerospace, dental, medical, and automotive. Most of the 3D printing process used wire or powder as raw materials which restrict the further usage of current techniques. In the work, a thin film-based Laser  $\mu$ -3D printing is deployed for the fabrication of triboelectric nanogenerator for harvesting waste vibration energy from surrounding.

With advancement in technologies, Laser decal transfer can be deployed for transfer of thin film over substrates are possible making it substrate independent. In present work laser decal transfer was used for the transfer of ZnO over Indium Tin Oxide with PDMS as a sacrificial layer. Further FEP sheet deposited with copper was used as a tribo-pair with ZnO. ZnO single track was printed at different laser fluence varied from 3.7 - 5.20J/cm<sup>2</sup> and at different pulse overlap (60%, 70%, 80%, 90%) with laser wavelength of 10.6  $\mu$ m. TENG fabricated with  $\mu$ - 3D printing and compare it with hydrothermal growth method to check its performance at same condition. This work also emphasizes on exploring the capacity of  $\mu$ -3D printing of ZnO ceramics with CO<sub>2</sub> laser for different pattern and structure.

The printed structure was analysed using SEM and optical micro graphs awhile the X-Ray diffraction is used for phase confirmation of growth ZnO nanostructures. The output of the TENGs was measured at different tapping rate and short circuit current and open circuit voltage is measured using electrometer and oscilloscope respectively.

# TABLE OF CONTENTS

## CHAPTER 1

### Introduction

1.1 Tribo-electric Nano-generators:	1
1.1.1 Mechanism Model of Tribo-electricity:	2
1.1.2 Modes of operation of TENG :	4
1.2 Motivation for the thesis:	9
1.2.1 Problem associated with Patterned deposition structure:	9
1.3 Aim of thesis and significant contribution	10
1.4 Organisation of thesis	10

## CHAPTER 2

### Literature review

2.1 Various Technique for fabricating TENG:	11
2.1.1 TENG fabrication using Physical Vapor Deposition (PVD):	11
2.1.2 TENG fabrication using Chemical Vapor Deposition (CVD):	13
2.1.3 TENG fabrication using Sol-Gel Method :	15
2.1.4 TENG fabrication using Electrochemical Deposition:	16
2.1.5 TENG using Hydrothermal method :	18
2.2 Device fabricated using $\mu$ -3D printer:	20
2.3 Research Gap	21

## CHAPTER 3

### Experimental setup

3.1 Feed stock Preparation for $\mu$ -3D printer :	22
3.1.1 Sacrificial layer coating on Silicon wafer:	22
3.1.2 Magnetron sputtering deposition:	24
3.1.3 $\mu$ - 3D printer	26

3.2 Characterization techniques:	28
3.2.1 X-Ray Diffraction	29
3.2.2 Field Emission Scanning Electron Microscopy (FESEM):	30
3.3 TENG Performance testing setup	31
3.3.1 Tribo Testing setup :	31
3.3.2 Current and Voltage measuring Setup :	32

## **CHAPTER 4**

### **Parametric investigation for 2D printing of ZnO structure for TENG application**

4.1 Influence of laser fluence on the track printed ZnO :	34
4.2 Influence of spot overlap on the track printed of ZnO:	35
4.3 Influence of growth temperature on the nanostructure ZnO steps:	36

## **CHAPTER 5**

### **TENG performance analysis**

5.1 Current and Voltage vs. Time Characteristics at various Tapping rate Rate:	40
5.2 Combined voltage vs Tapping rate and Current vs Tapping rate graphs	42
5.3 XRD plot of ZnO deposited on silicon wafer and ZnO deposited on ITO coated glass	43
5.4 Adhesion characteristics of grown and printed sample with or without substrate heating	44

## **CHAPTER 6**

### **Future scope of work and conclusion**

6.1 Conclusions	48
6.2 Future scope of work:	49

## TABLE OF FIGURES

Serial no.	Title	Pg.no.
	Figure 1.1 Block Diagram of TENG Energy Harvesting System	1
	Figure 1.2 Mechanism of TENG	2
	Figure 1.3 Contact Separation Mode	5
	Figure 1.4 Sliding mode of operation.	6
	Figure 1.5 Single electrode mode of operation	7
	Figure 1.6 Free standing mode of operation	8
	Figure 2.1 (a) Paper based Teng with Cu deposited using PVD (b) Cu deposited on Kapton Polyimide (c) Al deposited onto pinned finger	12
	Figure 2.2 (a) Schematic of TENG between Graphene/PET (b) process of fabrication of layer of Graphene (c) schematic of TENG between ITO and MoS <sub>2</sub>	13
	Figure 2.3 (a) Schematic fabrication process of PUA. (b) Fabricated PUA-TENG(c)Schematic illustration of the TENG made of CNF/PEI aerogel film paired with PVDF nanofiber mats	15
	Figure 2.4 Vertical grown Nano rods by ECD	16
	Figure 2.5 Schematic of Teng fabricated between PPy-PVDF	17
	Figure 2.6 ZnO nanosheets array SEM image, (b) schematic view of TENG device	18
	Figure 2.7 Strain gauge printed using $\mu$ -3D printer	20
	Figure 3.1 process of Donor substrate deposition	22
	Figure 3.2 Possible Deposition methods	22

Figure 3.3 Spin coater and PDMS coated silicon wafer	23
Figure 3.4 Schematic of sputtering	25
Figure 3.5 Sputtering Deposition unit	25
Figure 3.6 variants of laser induced transfer process	26
Figure 3.7 $\mu$ -3D Printer	27
Figure 3.8 Bragg's diffraction law	29
Figure 3.9 X-ray diffraction unit	29
Figure 3.10 FESEM	30
Figure 3.11 Tribo-tapping setup	32
Figure 3.12 oscilloscope and Electrometer	32
Figure 3.13 TENG circuit	33
Figure 4.1 Track deposition at varying laser fluences	34
Figure 4.2 Track Deposition at varying overlap percentage	35
Figure 4.3 Hydrothermal Growth process	36
Figure 4.4 SEM micrographs of varying growth	36
Figure 5.1 Multilayer schematic for TENG device	38
Figure 5.2 ZnO printed on ITO coated glass with fabricated device	40
Figure 5.3 Voltage vs. time at varied tapping rate	40
Figure 5.4 Current vs. time at varied tapping rate	41
Figure 5.5 Current Graph	42
Figure 5.6 Voltage Graph	42
Figure 5.7 XRD plot for ZnO donor	43

Figure 5.8 XRD plot for ZnO Printed on ITO coated Glass	43
Figure 5.9 Scotch Tape test	45
Figure 5.10 Image J analysis process	45
Figure 5.11 grain selection during image analysis	46

## LIST OF TABLES

<b>Serial no.</b>	<b>Title</b>	<b>Pg.no.</b>
	Table 3.1 Machine specification	27
	Table 5.1 Image analysis testing result	46

## ACRONYM

**S.no.      Acronym                      Expansion**

1	IoT	Internet of Things
2	TENG	Triboelectric nanogenerator
3	ZnO	Zinc Oxide
4	FEP	fluorinated ethylene propylene
5	ITO	Indium tin oxide
6	PVD	Physical Vapor Deposition
7	CVD	Chemical Vapor Deposition
8	ALD	Atomic Layer Deposition
9	PDMS	Polydimethylsiloxane
10	SMA	Shape Memory Alloy
11	Ni-Ti	Nickel Titanium alloy
12	RF sputtering	Radio Frequency sputtering
13	LIFT	Laser induced forward transfer
14	CO <sub>2</sub>	Carbon Dioxide
15	Nd:YAG	Neodymium-doped yttrium aluminum garnet
16	KMnO <sub>4</sub>	Potassium permanganate
17	RPM	Repetition per minute
18	ECD	Electrochemical deposition

# Chapter 1

## Introduction

### 1.1 Tribo-electric Nano-generators:

With rapid development of IoT, the count of sensors used in IoT is expected to increase around about 150 billion by 2025. Thus, sustainable energy supplies without recharging and replacement of charge storage devices have its own importance in growing market. Among the various energy harvesting units available, 1.1 Tribo-electric Nano-generators (TENG) has attracted greater attention due to high output power and voltage, wide range of materials from organic to inorganic, eco-friendly and inexpensive fabrication process. Three types of operational modes are available which includes contact-separation mode, sliding mode and free-standing mode are widely used and studied.

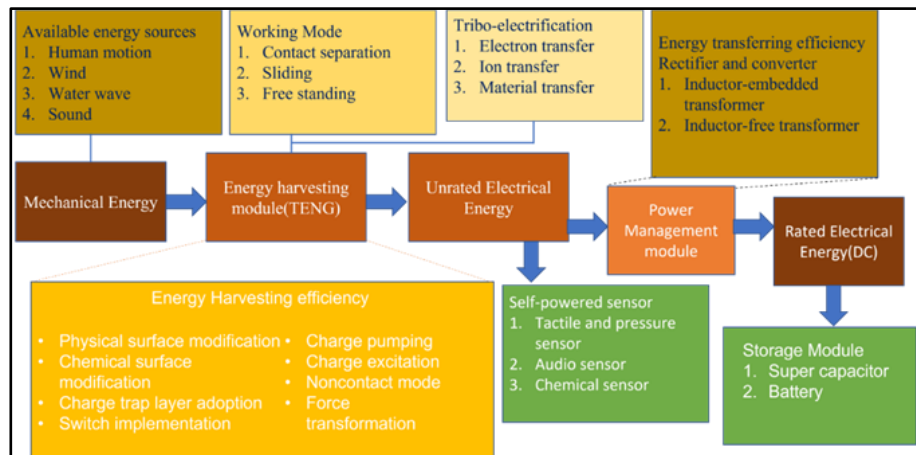


**Figure 1.1** Block Diagram of TENG Energy Harvesting System

Figure 1.1 shows the block diagram of TENG based energy harvesting system where from the available energy sources which might be wind or water, or human motion. It is based on the working mode chosen and the tribo-electrification that happens in the process. The energy generated during the process requires energy to be transferred either through inductor-embedded transformer or inductor-free transformer. It is however noted that the energy generated is normally unrated electrical energy which needs a proper conversion to rated energy using a suitable

power management module. Self-powered sensors which include tactile and pressure sensor, audio sensors or chemical sensors can be energized using power generated from tribo setup in its unrated energy form as well.

The output power obtained in TENG has its dependency on magnitude of tribo-electrification happening during the process. Therefore, it becomes highly important to select a comprehensive set of tribo materials such that tribo-electrification can be increased. In the process of tribo-electrification, apart from tribo-electrification, the principle of electrostatic induction plays a major role which is simply redistribution of electric charge in the object due to influence of nearby charged objects. The mechanism of tribo electrification is challenging concept and hence based on various models with theory centring around electron transfer model, ion transfer model, material transfer model is being followed. The models are well explained in chapter of literature survey.

Based on the above discussion, the study is focused on developing tribo-electric nanogenerator where energy can be generated using Zinc Oxide thin film both with and without growth as Tribo-positive layer and FEP (fluorinated ethylene propylene) as Tribo-negative layer.

### 1.1.1 Mechanism Model of Tribo-electricity:

Mechanism of tribo-electricity[1]:

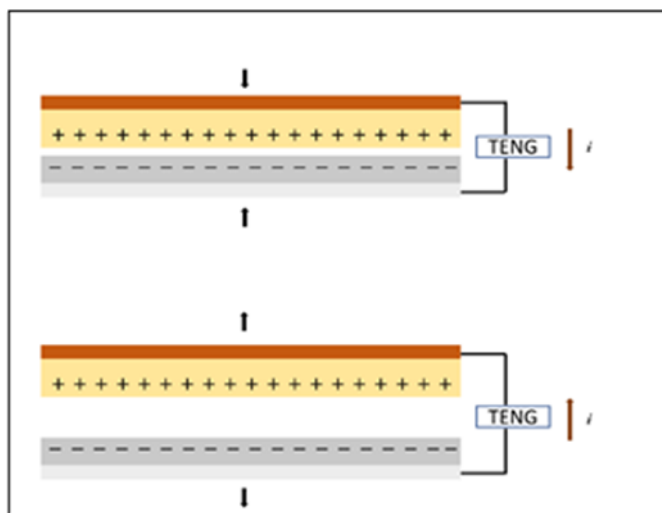


Figure 1.2 Mechanism of TENG

There are two important parameters i.e., tribo-electrification and electrostatic charge induction that concludes the working of TENG. It is however noted that most of the research in the field is concentrated on tribo-electric charge interaction between two solid bodies. It is however even till date a challenge with which charge species transfer during tribo-electrification, especially between non-ionic contacts as observed by Shepelin et al. [1]. Therefore, different models were floated to study the experimental results. For optimum selection of material, it essentially follows tribo-electric series based on experiments however it lacks solid theoretical evidence and hence is a challenge to accept it as a principle series.

Multiple models have been the basis of triboelectric study and the series established which is discussed here.

**i. Electron transfer model**

As discovered by Shepelin et al. [1], the initial concept for tribo-electric nano-generation is based on surface trap at insulator-insulator and metal-insulator contact pairings. Based on their experimental findings, they hypothesised that the work function and fermi level define a material's tribo-electric characteristics. Since the band gap is greater for insulators than semiconductors, electron transmission in the former is more challenging. The observed tribo-electric charge density is much lower than the trapped electron density as determined by the experiment. Some examples of experimental proof of electron transfers occurring during metal-insulator tribo-electrification were same author. At the surface, there is additional evidence of thermionic emission and photoelectron emission.

**ii. Ion Transfer Model**

Apart from electron transfer model, mobile ion gets transfer from one material to another material during contact between tribo-positive and tribo-negative surfaces. MaCarthy et al.[2] suggested in his work that ions are asymmetrically separated and contributes to tribo-electric

charge. The concept of ionic charge transfer is extended to non-ionic polymers as well. It is observed that two materials of different ionic charges when comes in contact exchanges electron and the vacant space has positive charge on one surface and negative on other. These charges take place in energy generation.

### **iii. Material transfer model and mechanochemistry:**

This model was not initially considered as a major mechanism when compared with already discussed models. Salaneck et al.[3] focused on correlating between charge transfer and material transfer however it was disputed whether the share in charge generation by the process has some significance or not. However, Baytekin et al.[4] found that polymer contact electrification may produce patterns of nanoscopic charges. Additionally, researchers hypothesised that electrons cause triboelectrification between insulating polymers.

#### **1.1.2 Modes of operation of TENG :**

##### **i. Contact separation mode**

As discussed by kim W et al.[5], The triboelectric effect is used by TENG, sometimes referred to as contact-separation triboelectric nanogenerators, as a method of energy harvesting. Triboelectric charging, which involves the production of static electricity through the contact and separation of several materials, is the basis for TENGs.

Two materials with various triboelectric characteristics are brought together and subsequently separated in the contact separation mode. When the materials come into contact, electrons go from one to the other, creating an unbalanced charge. The charge imbalance causes an electric potential difference when the materials separate, which produces an electric current. To maximise the triboelectric effect, these materials can be chosen based on their electron affinities and work functions.

The electrode, which typically consists of a conductive material, gathers the produced charges, and permits the movement of electric current.

Depending on the TENG design, the electrode may be positioned on either one or both sides of the triboelectric layer. Electricity produced can be used to power electronic equipment and sensors or stored in capacitors.

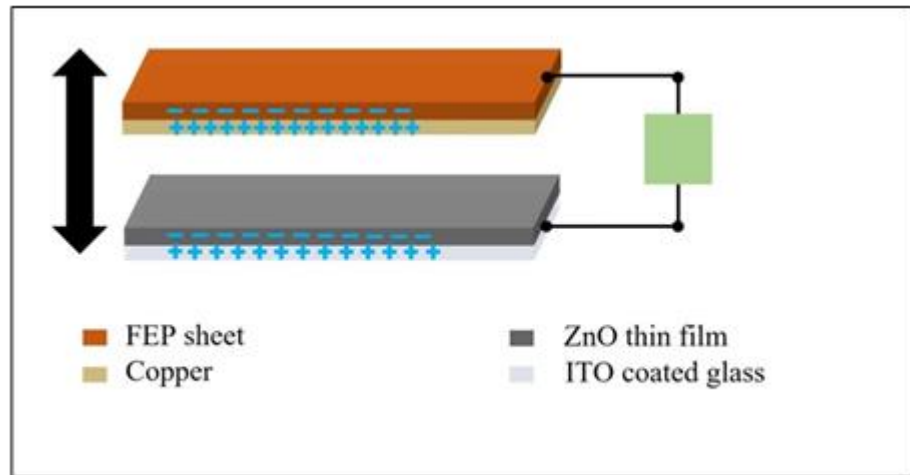


**Figure 1.3 Contact Separation Mode**

Applications involving vertical movements, such as walking or vibration, are ideal for Contact Separation TENGs.

ii. **Linear sliding mode**

Another operational mode of a Triboelectric Nanogenerator (TENG) as discussed by Lin Z et al. [6], allows for energy collection via relative linear motion between two contacting surfaces. The TENG generates electricity in this mode by using the triboelectric effect and electrostatic induction. An electrode and a triboelectric layer make up the two primary parts of a linear sliding mode TENG. Two materials with differing triboelectric characteristics make create the layer that is triboelectric. The ability of these materials to produce opposing charges upon contact and separation from one another is the basis for their selection.

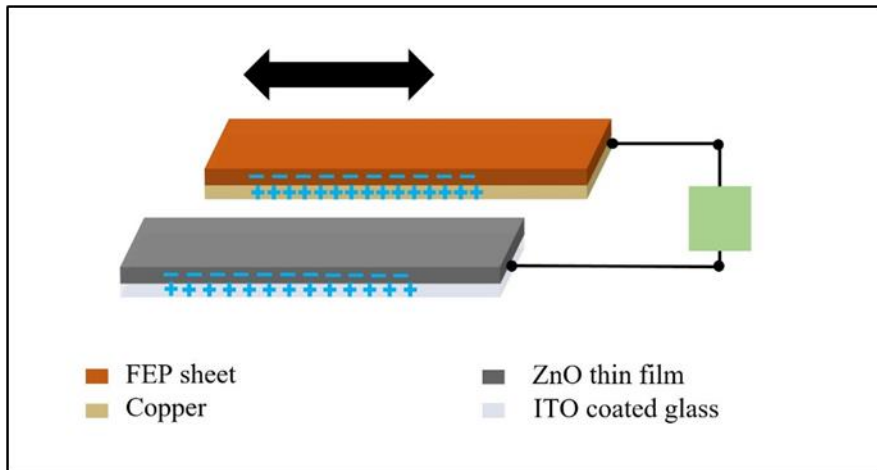


**Figure 1.4 Sliding mode of operation.**

The triboelectric effect causes electrons to move between the two sides of the triboelectric layer when they come into contact, creating static charges on the surfaces. The triboelectric layer repeatedly contacts and separates from the surfaces when relative linear motion takes place between them. An electrical current is produced due to redistribution of charges and the associated electric potential difference.

The electrode, which is normally constructed of a conductive material, is utilised to collect the created charges and to enable the passage of electricity. Depending on the TENG design, the electrode may be positioned on either one or both sides of the triboelectric layer.

Sliding mode TENGs have demonstrated energy harvesting capacity from mechanical motions like sliding or reciprocating motions:

### **iii. Single-electrode mode**

A Triboelectric Nanogenerator's (TENG) single-electrode mode is an operational mode that enables energy harvesting with a single electrode. It is a different configuration from the dual-electrode mode, which is frequently utilised and uses two different electrodes. The TENG structure is made simpler by the single-electrode mode, which also has advantages in some applications.

A triboelectric layer and a single electrode make up the device in the single-electrode mode of TENG. Usually, two distinct materials with

opposing triboelectric characteristics make up the triboelectric layer. The triboelectric effect produces charges on the surfaces of these materials when they come into contact and separate from one another as a result of mechanical motion from outside the system.

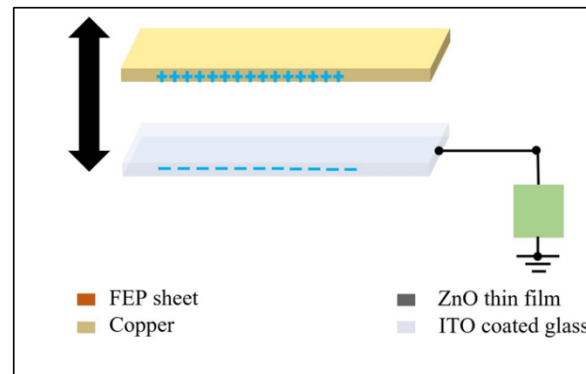


**Figure 1.5 Single electrode mode of operation**

The single-electrode mode employs a single electrode to both collect and redistribute the charges, as opposed to the dual-electrode mode, which uses two distinct electrodes to gather charges of opposite polarities. Typically, the single electrode is wired to a load or energy storage device, like a capacitor or battery. The produced charges from the triboelectric layer's contact and separation are gathered by a single electrode, which results in an electric potential difference and an electrical current.

TENG's single-electrode mode has benefits such as easier device manufacture, less complexity, and perhaps higher power output. It does away with the requirement for a separate counter electrode, simplifying the device's structure and lowering its size and weight. Additionally, by reducing electrical resistance in the circuit, the absence of a counter electrode may result in a higher power output and greater efficiency.

It's crucial to remember that the choice between single-electrode and dual-electrode modes depends on the application requirements and the required TENG performance characteristics. When it is difficult to create dual-electrode structures or when a small design is required, Single electrode TENGs are very helpful.

#### iv. Free-standing mode

A TENG free-standing mode is an operational mode that enables energy harvesting without the requirement for an external mechanical restraint or a supporting substrate. In terms of TENG design and applications, it is a special configuration that enables adaptability and versatility.

The triboelectric layer is self-supporting and free to move or deform in response to mechanical or environmental stimuli when the TENG is in the free-standing state. The creation and application of TENGs can be done with more freedom because there is no substrate or mechanical restriction. An electrode or electrodes, a protective encapsulation, and a triboelectric layer are the standard components of a free-standing mode TENG. The formation of charges when two materials come into contact and then separate is made possible by the triboelectric layer, which is made up of two distinct materials having divergent triboelectric characteristics.

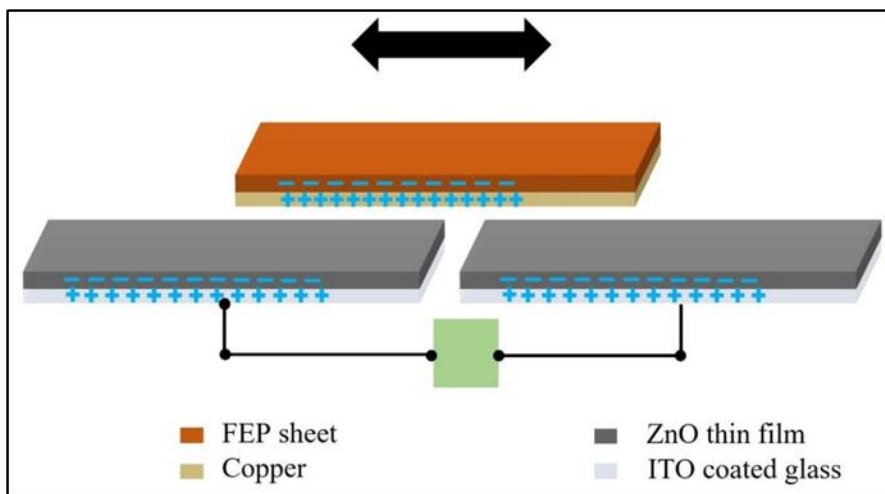


Figure 1.6 Free standing mode of operation

The electrodes serve to collect the produced charges and enable the flow of electric current. They are positioned on the opposing sides of the triboelectric layer. The TENG is protected by the protective capsule against environmental elements including moisture, dust, or mechanical harm.

The triboelectric layer can move or deform in the free-standing mode in response to a variety of mechanical stimuli, such as vibrations, bending, twisting, or stretching. The triboelectric materials are brought into touch and then separated by this movement, which causes electrical charges to form and ultimately transform mechanical energy into electrical energy.

TENG's free-standing configuration has a number of benefits. It makes it possible to create flexible, conformable electronics that fit into a variety of form factors and curved surfaces. Additionally, it enables the collection of energy from a variety of mechanical movements or environmental deformations. Additionally, the lack of a supporting substrate makes the device production process simpler and might even increase the TENG's power output and efficiency. It provides chances for energy harvesting in circumstances when conventional rigid or limited TENG setups might not be suitable. Free-TENGs are useful for extracting energy from airflow or ambient vibrations and may be employed in portable or wearable electronics.

## **1.2 Motivation for the thesis:**

The present literature shows the fabrication of laser decal transfer based TENG using which paves a way for mask less printing process.

### **1.2.1 Problem associated with Patterned deposition structure[7], [8]:**

- High mask fabrication cost
- Design freedom is limited that will increase the production time.
- Multilayer deposition of thin film becomes difficult.
- Material freedom is less.
- Thickness control and internal chemistry becomes somewhat complicated.

## **1.3 Aim of thesis and significant contribution**

This project deals with the fabrication of a smart device with a novel  $\mu$ -3D printing technique which involves Laser Decal transfer where laser does not interact with the material being printed. Hence the printing of material is without any physical or chemical change. Here ZnO being

transferred as in pattern structure to improve the output of the TENG device. Laser  $\mu$ -3D printing significantly enhance the output of TENG compare to hydrothermal fabricated TENG. Hence It will be delta change increment towards a green energy harvesting.

#### **1.4 Organisation of thesis**

- Chapter 1 gives a brief introduction about the type of device fabricated and physics involved in its working.
- Chapter 2 talks about the study of same device fabricated using other techniques which gives more idea about the existing output and difficult faced by the process.
- Chapter 3 gives a detailed description of devices and facility used in the process of fabrication of device from the fabrication phase to performance phase.
- Chapter 4 deals with the process of parameter optimisation from printing pattern to growing nanostructures.
- Chapter 5 deals with the characterization of the device for confirming material and then testing performance of device.
- Chapter 6 deals with the work possible left in the present way and conclusion of the whole project.

## Chapter 2

---

### Literature review

A layer of material with a thickness between a nanometre and a micrometre is referred to as a thin film. In many different industries, including electronics, optoelectronics, photovoltaics, coatings, and sensors, thin films are often utilised. When compared to bulk materials, thin films have various benefits. By adjusting the deposition settings and surface treatments, thin films may be designed to have certain surface characteristics, such as smoothness, roughness, or chemical functionality. Thin films' special qualities, such their high surface-to-volume ratio, can improve performance in a variety of applications. For instance, compared to conventional bulk transistors, thin film transistors (TFTs) offer more mobility and quicker switching rates. Depending on the intended use, thin films can be designed to have certain characteristics like electrical conductivity, optical transparency, magnetic behaviour, or mechanical flexibility.

In addition, ZnO thin films have been used for sensing applications, such as temperature sensor, Gas sensor, humidity sensors, and biosensors, due to their high sensitivity and selectivity to various analytes. ZnO thin films have also been investigated for their potential application in energy-related fields, such as solar cells and energy storage devices.

Overall, the use of ZnO thin films in optoelectronics, electronics, and sensing devices has shown great potential for various applications, and on-going research continues to explore and improve the properties and performance of ZnO thin films for these applications.

#### **2.1 Various Technique for fabricating TENG:**

##### **2.1.1 TENG fabrication using Physical Vapor Deposition (PVD):**

The aim is often a pure and high-quality solid ZnO material. Deposition Methods: Thermal evaporation and sputtering are two

methods that may be used in the PVD deposition process for ZnO thin films.

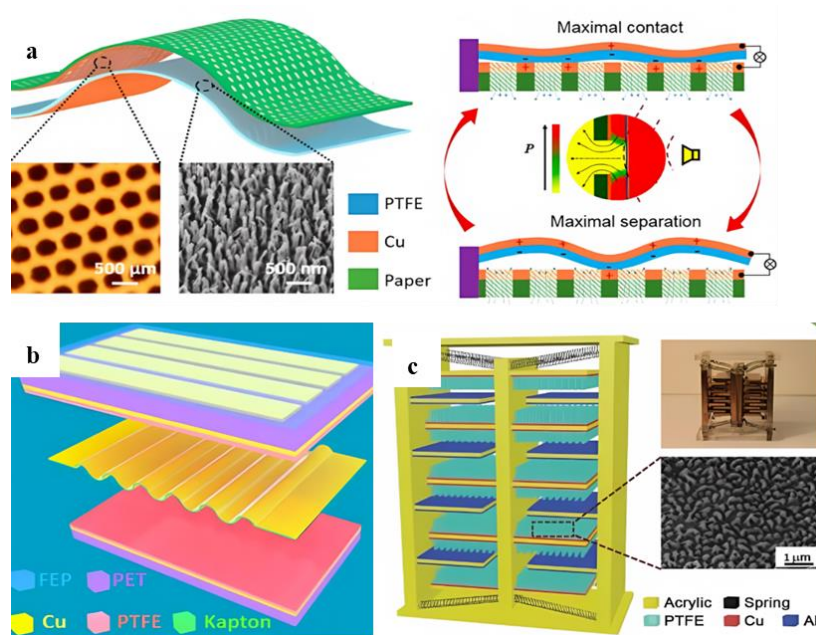


**Figure 2.1** (a) Paper based TENG with Cu deposited using PVD[9] (b) Cu deposited on Kapton Polyimide[10] (c) Al deposited onto pinned finger[10]

Xinlong Huang et al. [9], fabricated TENG by using PVD process where tribo pair was between the paper and copper deposited using PVD process and the open circuit voltage achieved was 400 V and low current was achieved, As stated by Yang W et al. [10] TENG fabricated TENG by PVD where Al being Tribo-Positive and PTFE being Tribo- Negative layer, Voltage was 300 V whereas short circuit current 200 μA, Yuanjie Su et al. [11] fabricated TENG with PVD technique between PTFE as Tribo- Negative layer, and copper as Tribo- Positive layer with voltage as 45 V and Current about 6 μA, Keun Young Lee et al. [12] fabricated a TENG between Copper deposited hemisphere array as Tribo- Positive layer and PTFE as Tribo- Negative layer Voltage drawn was 25 V and short circuit current being 2 μA.

in One technique used to deposit zinc oxide (ZnO) thin films for Triboelectric Nanogenerator (TENG) applications is PVD (Physical Vapour Deposition). An outline of the PVD procedure for creating ZnO thin films in TENGs is given below:

Thermal evaporation is a technique that involves heating a ZnO target to a high temperature, which causes the ZnO material to vaporise. The ZnO vapour then cools and condenses, creating a thin coating on the substrate. To enable deposition, the substrate is often positioned near to the target.

Sputtering is the process of ejecting atoms and molecules from the ZnO target surface by hitting it with high-energy ions. The ZnO thin film is subsequently created by the deposition of these ejected species onto the substrate. Techniques like DC sputtering or RF sputtering can be used to perform sputtering. As the ZnO vapour or other species are expelled from the target during the deposition process, they slowly adhere to the substrate and form thin films.

### 2.1.2 TENG fabrication using Chemical Vapor Deposition (CVD):

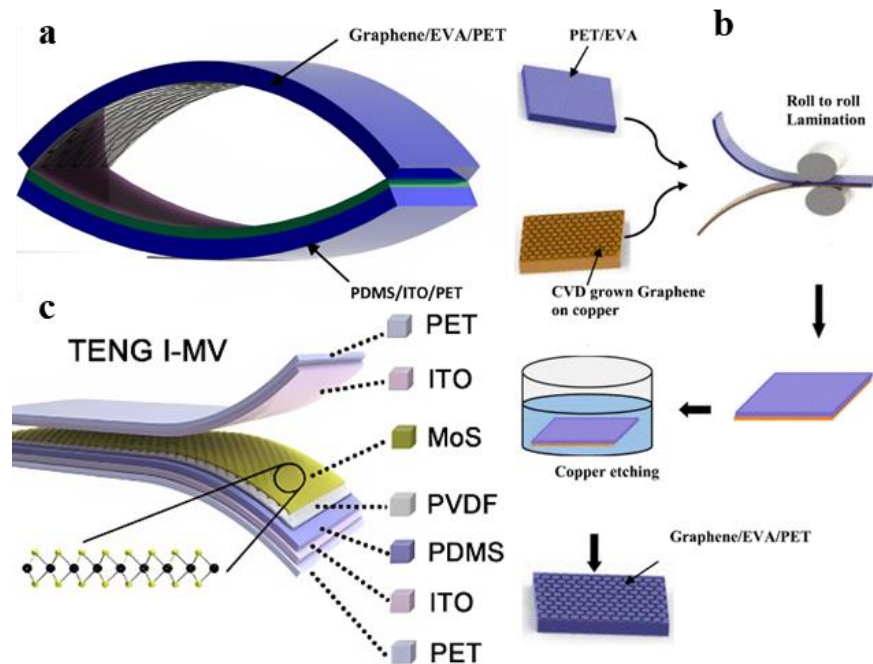


**Figure 2.2** (a) Schematic of TENG between Graphene/PET[14] (b) process of fabrication of layer of Graphene (c) schematic of TENG between ITO and MoS<sub>2</sub>[14]

Xinlong Huang et al.[13] fabricated the TENG using CVD where MoS<sub>2</sub> as Tribo-negative layer and ITO Tribo-Positive layer where peak to peak Voltage achieved was 8V here graphene was coated on graphene,B.N. Chandrashekar et al. [14] fabricated TENG using PDMS as Tribo-negative layer and Graphene as Tribo-Positive layer with peak to peak

Voltage as 20V and Current as 1 $\mu$ A, Saeed Ahmed Khan et al. [15] fabricated TENG using CVD with Carbon Nanotube as Tribo- positive layer and PTFE as Tribo-negative layer and Voltage obtained was 25 V and Current as 1  $\mu$ A.

High-quality zinc oxide (ZnO) thin films are deposited with CVD method. It provides great film homogeneity and exact control over film growth. The following are some important details of CVD-based ZnO thin film deposition:

In regulated environments, precursor gases react chemically to produce ZnO thin films. The reaction chamber is filled with precursor gases containing zinc and oxygen, such as zinc acetate or diethyl zinc. The precursors go through chemical processes that result in the deposition of ZnO onto a heated substrate. Typically, the reaction takes place at high temperatures between a few hundred and several hundred degrees Celsius. The reaction between the ZnO species produced in the gas phase and the substrate surface leads to the development of a ZnO thin film. By altering the precursor flow rates and deposition duration, the film thickness may be managed.

Different types of CVD procedures may be used for the formation of ZnO thin films, including:

- a. Atmospheric Pressure CVD (APCVD) is a reasonably straightforward technology that operates at atmospheric pressure. It is appropriate for large-area deposition but could produce films of inferior quality than with other CVD techniques.
- b. Low-Pressure CVD (LPCVD): This kind of CVD works best at pressures between a few and several hundred millibars. It can produce extremely crystalline ZnO films and gives users more control over film quality.
- c. Plasma-Enhanced CVD (PECVD): PECVD uses plasma to speed up the precursor gases' breakdown and reaction. Lowering the deposition

temperature and improving film quality are also benefits of plasma activation.

### 2.1.3 TENG fabrication using Sol-Gel Method :

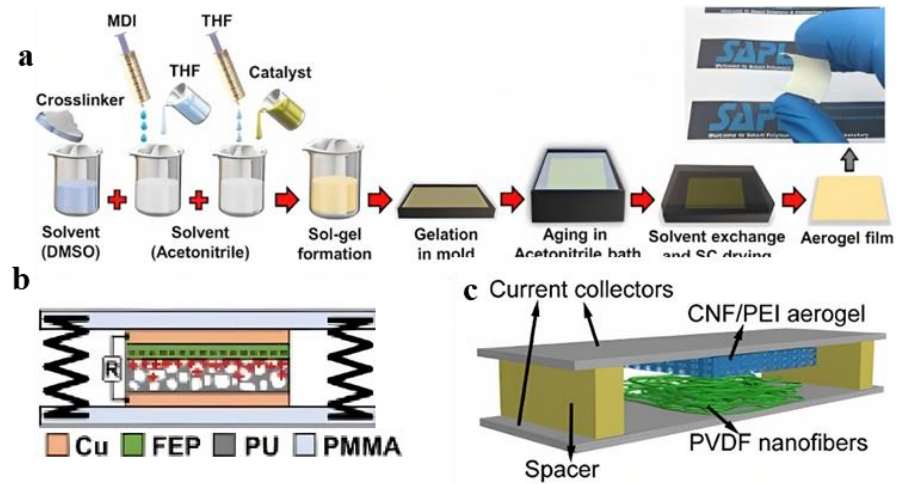


**Figure 2.3** (a) Schematic fabrication process of PUA.[16] (b) Fabricated PUA-TENG[16] (c)Schematic illustration of the TENG made of CNF/PEI aerogel film paired with PVDF nanofiber mats[17]

A Sahu M et al. [16] fabricated a TENG device using sol-Gel method to obtain tribo pair between FEP and PU sheet voltage and current obtained was 300 V and 2.2  $\mu\text{A}$  and 5.5  $\mu\text{W}/\text{cm}^2$ , Sheng-Ji Wang et al.[17] fabricated a TENG based on Sol- gel method where Tribo-pair was between CNF as Tribo-Positive layer and PVDF as Tribo-negative layer with voltage as 250 V and current as 25  $\mu\text{A}$ , Wei Xu et al. [18] fabricated a TENG device which was between Nickel fabric Electrode moving and as PDMS and Al Tribo- pair with 200V voltage and 20  $\mu\text{A}$  output.

A Triboelectric Nanogenerator (TENG) device that uses zinc oxide (ZnO) nanoparticles made using the sol-gel process is referred to as a sol-gel ZnO-based TENG. TENGs are an energy harvesting technique that transforms mechanical energy, like motion or vibration, into electrical energy. The versatile sol-gel method is used to create a variety of materials, including ZnO nanoparticles. This procedure involves creating a precursor solution containing ZnO, which then goes through condensation and hydrolysis reactions to form a gel. After that, the gel is dried and calcined to produce ZnO nanoparticles. Sol-gel ZnO

nanoparticles are commonly employed as the active substance in one of the triboelectric layers when incorporated into a TENG device. The transfer of electrons between two distinct materials that come into touch and then are separated causes the triboelectric effect. Depending on its characteristics and how it is combined with other materials in a sol-gel ZnO-based TENG, the ZnO layer can function as either the positive or negative triboelectric material.

The sol-gel ZnO-based TENG produces an electrical output when mechanical motion or deformation like pressing, bending, or vibration takes place due to the triboelectric effect. The generated electricity can be captured and used for a variety of tasks, including recharging batteries or powering handheld electronics. The benefits of ZnO nanoparticles, including as their high surface area, superior electrical characteristics, and possibility for low-cost production, have drawn attention to sol-gel ZnO-based TENGs. Sol-gel ZnO-based TENGs are a potential method for sustainable and effective energy harvesting from mechanical sources.

#### 2.1.4 TENG fabrication using Electrochemical Deposition:

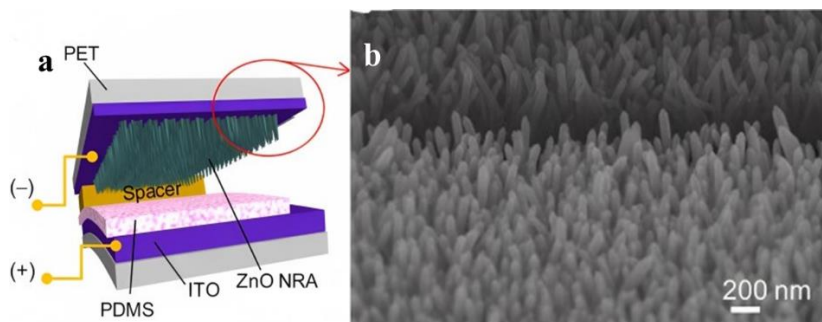
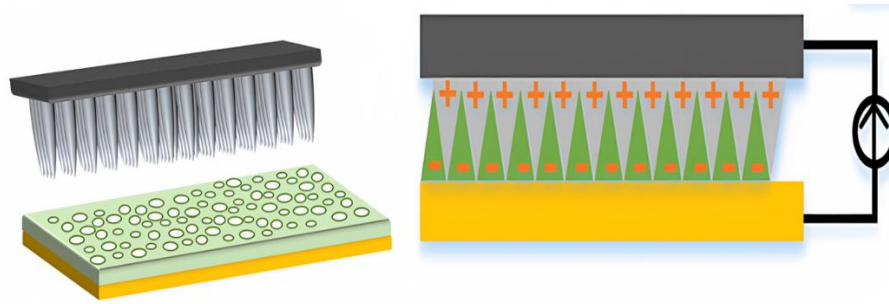


Figure 2.4 Vertical grown Nano rods by ECD[19]



**Figure 2.5 Schematic of TENG fabricated between PPy-PVDF[20]**

Yeong Hwan Ko et al.[19] Fabricated a TENG device using ECD process with tribo-pair between PDMS as tribo-negative layer and ZnO NRA as tribo-positive layer with performance touching 6V as peak to peak Voltage and peak current as 60 nA. Honghao Zhang et al. [20] fabricated a TENG device with same process with tribo-pair between PPy as tribo-positive and PVDF as tribo-negative layer, short circuit and open circuit voltage reach was 20 V and 1.5  $\mu$ A

The technique of depositing thin films of different materials onto surfaces is known as electrochemical deposition, or ECD. These thin films can be used in TENGs for a variety of functions, including enhancing triboelectric characteristics, functioning as electrode materials, or promoting electrochemical processes. Using electrochemical deposition (ECD), metal oxides, such zinc oxide (ZnO) or titanium dioxide ( $\text{TiO}_2$ ), can be deposited as thin films. By offering a large surface area for triboelectric charging and producing a greater output voltage, these thin films can improve the triboelectric characteristics of the TENG. Metal oxide thin films can also function in the TENG structure as a semiconducting layer, aiding the passage of charge during the electrochemical processes. Conductive polymer thin films may be electrochemically deposited as thin films over TENG substrates and include polypyrrole (PPy) and polyaniline (PANI). When the TENG is operating, these thin coatings can serve as pliable, conductive electrodes, facilitating effective charge transfer. Conductive polymer thin films are ideal for wearable TENG applications because they are flexible, lightweight, and compatible with a variety of

substrates. On TENG substrates, ECD may be used to deposit thin films of metals like gold (Au) or platinum (Pt). These metallic thin sheets can act as electrodes in the TENG device, enabling effective charge collection and transfer. Additionally, the metal thin films can function as electrochemical reaction catalysts, enhancing the TENG's overall performance.

### 2.1.5 TENG using Hydrothermal method :

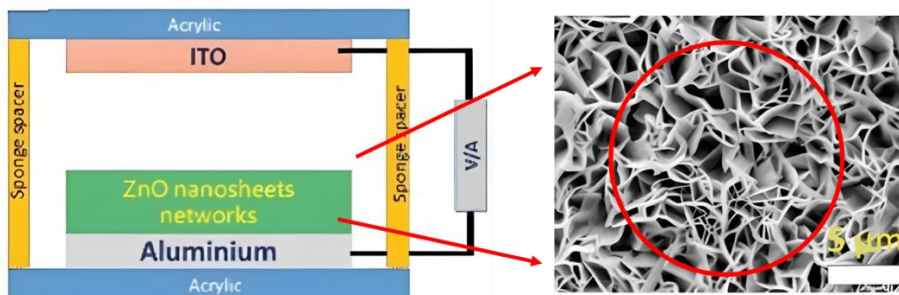


Figure 2.6 ZnO nanosheets array SEM image,[21] (b) schematic view of TENG device[21]

P.Supraja et al. [21] fabricated ZnO Nanosheets based TENG device with hydrothermal process with different tribo pair combination like ZnO- Polyimide, ZnO ITO. The short-circuit current and Open circuit voltage achieved was 5 V and 10  $\mu$ A. Performance was analysed at different loading condition by Manisha Sahu et al. [22] Teng was fabricated between ZnO as Tribo-positive layer and Polyimide Ar doped as Tribo-negative layer with 10 V voltage and 0.2  $\mu$ A current, As stated by Huidrom Hemojit Singh et al.[23] where TENG was between ZnO-PVDF as Tribo-positive layer and PTFE as Tribo-negative layer with 100 V and 1  $\mu$ A output.

By growing ZnO nanostructures in an aqueous solution at high temperatures and pressures, the hydrothermal approach can be used to create zinc oxide (ZnO) based Triboelectric Nano generators (TENGs). The hydrothermal process is simple, inexpensive, and capable of creating high-quality nanostructures with precise shape, which are all benefits for ZnO-based TENG fabrication.

The general description of the hydrothermal procedure used to fabricate ZnO-based TENGs. To encourage the nucleation and growth of ZnO nanostructures, a seed layer is typically put on a substrate, such as glass or silicon. Techniques including spin coating, sputtering, or physical vapour deposition can be used to build the seed layer. A appropriate zinc salt, such as zinc nitrate or zinc acetate, is dissolved in a solvent, frequently combined with additional additions like surfactants or pH adjusters. This creates a hydrothermal solution. The content and concentration of the solution can be changed to regulate the ZnO nanostructures' form and rate of growth. A high-pressure reaction vessel, like an autoclave, is used to hold the prepared hydrothermal solution. The hydrothermal solution is added to the substrate with the seed layer, which is then submerged, and the reaction vessel is then sealed and heated to a set temperature, usually between 80 and 200 degrees Celsius. ZnO nanostructures on the substrate are encouraged to grow in a regulated manner by the elevated temperature and pressure. After the hydrothermal growth, the samples are typically cleaned and washed to get rid of any contaminants or reactants that may have remained. To obtain high-purity ZnO nanostructures, this procedure is essential. The substrate surface is often used to pattern the electrodes using methods like photolithography, evaporation, or screen printing to collect the triboelectric charges produced during operation.

The TENG device is put together by combining ZnO nanostructures with a complimentary substance, such as a polymer that has various triboelectric characteristics, after the electrodes have been made. The two materials' alignment and contact are crucial for effective charge transfer during triboelectric interactions.

Numerous research publications have investigated the growth parameters, morphological control, device performance, and applications of ZnO-based TENGs made utilising the hydrothermal process. Different ZnO nanostructures, such as nanowires, nanorods, nanoflowers, and nanosheets, can be grown using the hydrothermal process and customised to meet the needs of TENG.

## 2.2 Device fabricated using $\mu$ -3D printer:

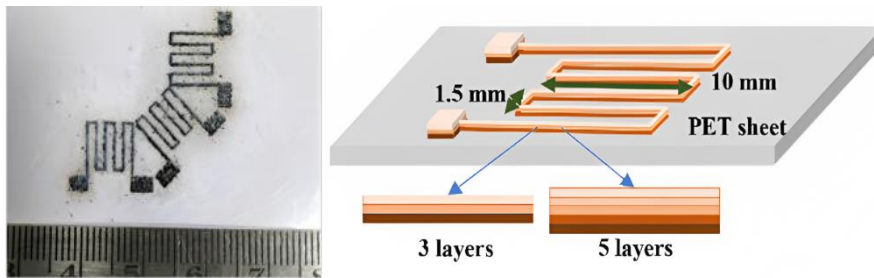


Figure 2.7 Strain gauge printed using  $\mu$ -3D printer[24]

A Sahu et al. [24] used Laser  $\mu$ - 3D printing to fabricate patterned thin film-based strain gauge with Nitinol SMA material. The material is printed in solid phase in pixel by pixel and layer by layer fashion to use pseudo elastic properties of nitinol for low strain rate applications.

Formed strain gauge from Ni-Ti was observed to be having advantage like tow- load sensing and was observed to have gauge factor within range 4-6 with varying number of layers gauge factors varied at the same time compared to commercial strain gauge factor of 2. For the sensor fabrication, design the strain gauge while taking into account the desired gauge factor, strain range, and mechanical characteristics of nitinol. Determine the dimensions and pattern of the strain gauge, including the sensing element and electrical connections. Nitinol thin film was used as the strain sensing material due to its pseudo elastic behaviour above room temperature. Nitinol donor thin film was fabricated on transparent substrate using physical vapour deposition systems. For printing of nitinol on flexible substrate the process parameters such as laser energy, pulse duration, focal point, and donor material properties is properly selected before the transfer process to achieve precise material transfer and preserve the pseudoplastic properties of Nitinol. With Laser  $\mu$ -3D printing the strain gauge patterned structure is printed on the flexible PET sheet for 5 number of layers to achieve a desired thickness. To measure the electromechanical response the electrical connections is made with copper wire with silver paste.

- **Advantages of using  $\mu$ -3D printer:**

Benefits are wide ranging from Design, high precision, selective deposition, rapid manufacturing, high material freedom. High freedom for design as anything that can be drawn with G & M codes can be made with  $\mu$ -3D printer. Its high-resolution printing with its low feature size and high controllability of motion results in high precision. For the micro sensor fabrication different material has individual functionality with respect to its location and thickness. Hence the  $\mu$ -3D printing provides the flexibility to print the material selectively at location with high precision. The laser  $\mu$ -3D printing has relatively less production time compared to above mentioned literature for the thin film fabrication techniques hence it can be used for the rapid prototyping in industrial stage for mass production.

Material independence: any substrate can be printed with this  $\mu$ -3D printer and can be varied with laser source.

### **2.3 Research Gap**

From above study it was found that thin films can be fabricated for TENG using any above techniques be it PVD, CVD or other and every technique has its own advantages and disadvantages. A novel method has also come in light recently where thin film of any intricacy can be made with ease without help of mask with avoids additional cost.

Above technique can be used for fabricating thin film TENG and study of its performance is required might higher performance observed

# Chapter 3

## Experimental setup

### 3.1 Feed stock Preparation for $\mu$ -3D printer :

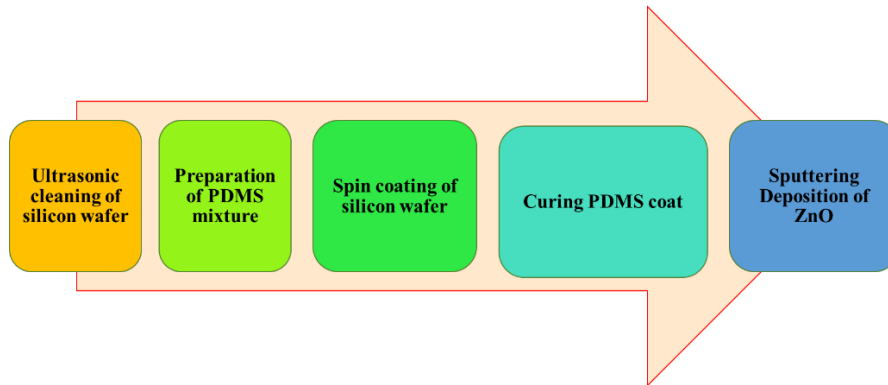


Figure 3.1 process of Donor substrate deposition

This work is focussing on fabrication of ZnO based TENG device with the above process adopted. First of all deposition of silicon wafer, single crystal (100) with ZnO is done by using RF Sputtering deposition.

There are various method that has been used for ZnO deposition they are:

Sputtering	PLD	Spray Pyrolysis	Sol Gel
<ul style="list-style-type: none"><li>• high Temperature plasma ion are used to remove material from the target and deposit it to donor</li></ul>	<ul style="list-style-type: none"><li>• pulsed laser in vaccumed ambience is used to erode of target material and deposit it</li></ul>	<ul style="list-style-type: none"><li>• here Zinc Nitrate solution is sprayed on very hot substrate</li></ul>	<ul style="list-style-type: none"><li>• repeated soaking of silicon wafer in Zinc solution and then drying</li></ul>

Figure 3.2 Possible Deposition methods

Here method most suitable to printing process has been adopted i.e. process that gives highest deposited area, best ZnO Crystal, and maximum control over deposition, on these parameters RF sputtering fits best.

#### 3.1.1 Sacrificial layer coating on Silicon wafer:

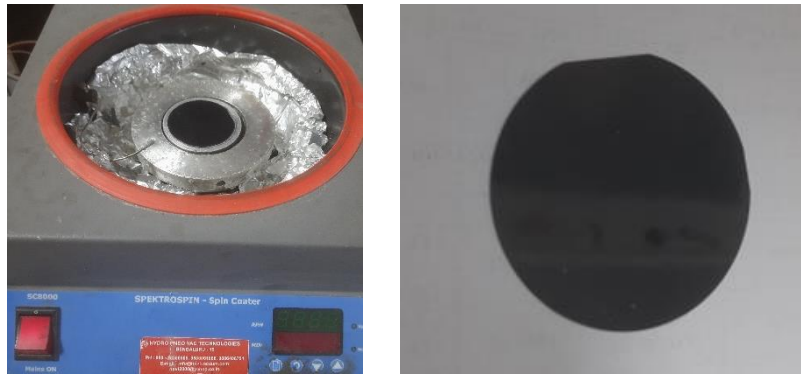


**Figure 3.3 Spin coater and PDMS coated silicon wafer**

The process of coating a silicon wafer with PDMS (Polydimethylsiloxane) a sacrificial layer typically involves the following steps:

1. **Cleaning silicon wafer:** Start by properly cleaning the silicon wafer to get rid of any impurities or contaminants. This may be accomplished by first cleaning it with an appropriate solvent, such as acetone or isopropyl alcohol, and then rinsing it with deionized water. Use a cleanroom air pump or clean nitrogen gas to dry the wafer. Silicon wafer was cleaned in ultrasonic cleaner up to 1 minute.
2. **Prepare the PDMS mixture:** A silicone elastomer known as PDMS is normally made up of a base polymer (PDMS A) and a curing agent (PDMS B). Mix the base polymer and curing agent in the specified 10:1 ratio to create the PDMS mixture. For the particular PDMS product you are using, adhere to the manufacturer's instructions.
3. **Degassing PDMS:** It's critical to eliminate any air bubbles that may have gotten stuck in the PDMS mixture after mixing. It is possible to do this by putting the mixture in a vacuum chamber and using vacuum (0.06MPa) for a certain amount of time (usually 30 minutes to an hour) to degas the PDMS. This process ensures a homogeneous and smooth coating.
4. **Apply PDMS on Silicon Wafer:** Pour the PDMS slurry cautiously over the silicon wafers centre once it has been gassed out. Spreads

the PDMS mixture uniformly across the wafer's surface using a clean pipette or a spin coater here spin coater (7000 RPM for over 10 minutes). If utilising a spin coater, you may change the spin speed and duration to get the appropriate thickness and uniformity.

5. **Remove Excess PDMS:** After covering the wafer, trim off any extra PDMS from the edges of the wafer using a fresh razor blade or a similar instrument. This facilitates the creation of smooth edges and stops undesired PDMS from interfering with following operations.
  
6. **Cure PDMS:** The PDMS elastomer has to cure on the covered silicon wafer in order to harden. The wafer is normally heated during the curing process in an oven or on a hotplate at a set temperature for a predetermined amount of time. Depending on the particular PDMS product, the curing temperature and duration might vary from a few hours to several hours (here curing has been done at 80°C for about 50 minutes).
  
7. **Cool and Store:** Allow the coated wafer to cool to room temperature once the PDMS has dried and hardened. Before using or treating the PDMS-coated wafer further, keep it in a clean, dust-free environment.

### **3.1.2 Magnetron sputtering deposition:**

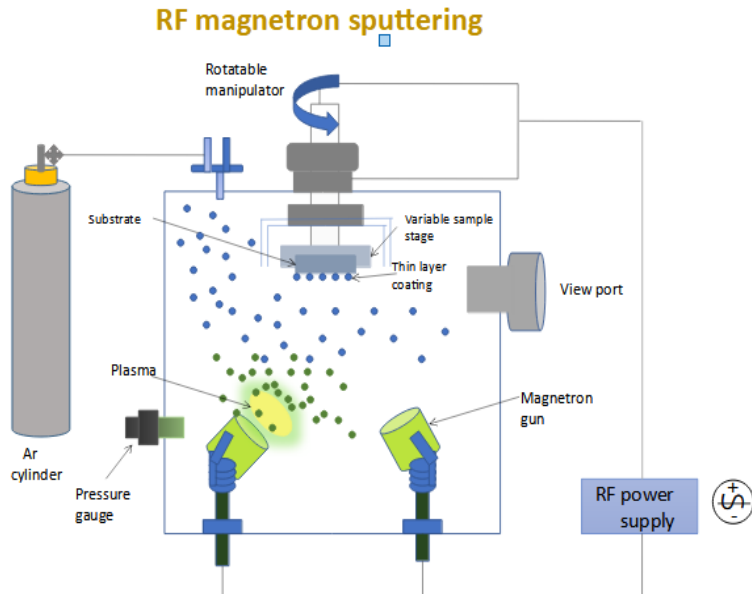


**Figure 3.4 Schematic of sputtering**



**Figure 3.5 Sputtering Deposition unit**

RF sputtering is a method where alternating electric potential is used in inert atmosphere at frequency equal to that of radio frequency, alternation of potential is done such that charge build-up is avoided which can result in arc formation in plasma which can result in quality issues or even can lead to stopping of the sputtering process.

A variant of sputtering process is DC sputtering which is used for the coating for electrical conductive material like Al, NiTi etc. but cannot help with dielectric material i.e. oxides or other.

When alternating electric potential is applied in the chamber gas in the chamber gets ionized, these ionized particle gets attracted to the surface on which coating has to be performed and as a result positive charge gets build up on the surface which is needed to be removed

Advantage of RF sputtering is that; plasma tends to spread throughout the deposition space rather than concentrating just on the cathode or anode pair. Arcing is avoided in this type of deposition where highly localised and energized discharge happen creating a build-up of charge at a specific Zone that causes a number of quality control issues.

Here created circular track on the surface of the target material is much spread and shallow, With pros there are cons that are, slow deposition rates requirement of higher Voltage, target being brittle more prone to breaking, Overheating becomes an issue here deposition was performed at 60 W for 45 minutes with substrate- plasma gun distance about 5 cm, substrate heating about 150° C , chamber pressure of about 300 Pa, Argon flow rate of 30 sccm After deposition using RF Sputtering there is printing using  $\mu$ - 3D printer with LIFT process.

### 3.1.3 $\mu$ - 3D printer

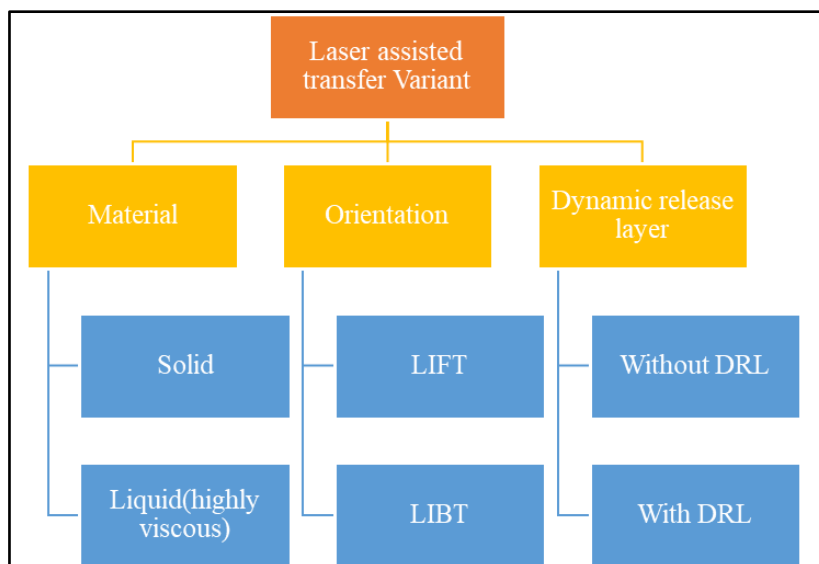


Figure 3.6 variants of laser induced transfer process

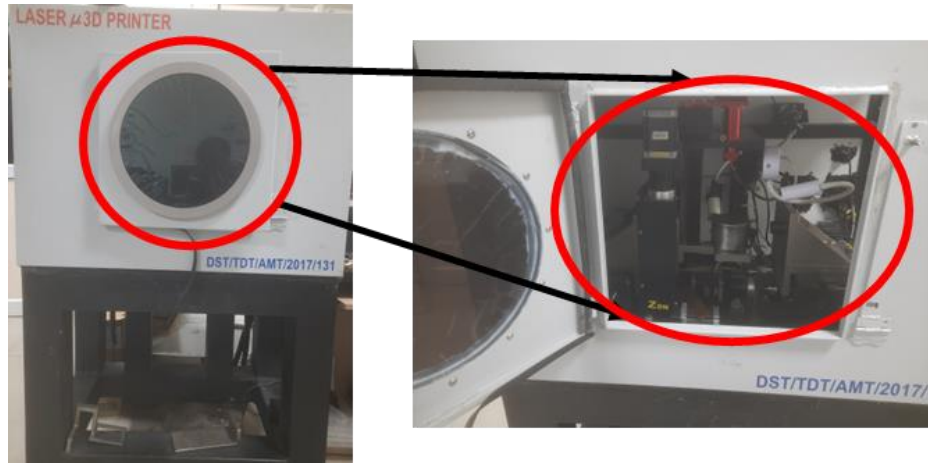


Figure 3.7  $\mu$ -3D Printer

**Micro 3D printer = LIFT with DRL + CNC control**

Parameter	Values
Laser Type	Pulsed Laser
Laser active Medium	CO <sub>2</sub>
Laser Wavelength	10.6 $\mu$ m
Shutter frequency range	0-25 kHz
Cooling type	Air Cooled
X-Y stage resolution	1 $\mu$ m

Table 3.1 Machine specification

**$\mu$ - 3D printer** : micro 3D printer is a device in which control system is deployed to control the variable of laser and motion of X-Y stage and can be said that it is a practical setup for LIFT method. It uses material transfer process of LIFT / LIBT with or without sacrificial layer.

LIFT with a Dynamic Release Layer has been used here for material transfer process which has the biggest merit of no phase change during material transfer

The donor substrate is covered with an absorbing, sacrificial layer known as the (DRL) dynamic release layer when the transfer material is transparent or laser sensitive material. DRL differs depending on the kind of laser used, for example, a CO<sub>2</sub> laser employs PDMS (organic material), which absorbs laser energy and causes the donor material to vaporise and provide enough propulsive force to expel the donor material. Nd:YAG lasers employ thin metal films, some of which use DRL; the thickness of the metal should be more than the laser's penetration depth (50-100 nm). Thin metal coatings like (Ti, Pt.) will alter depending on the substance to be coated. Here, no phase shift is seen in the flyer, and the photo-decomposing (PDP) polymer degrades synchronously. Shock wave production, a drawback of PDP, damages flyer material when it comes into contact with it.

Fragile materials including polystyrene, polyethylenimine, and polyepichlorhydrine are best transferred using this technique.

### **Process Parameters**

In the process used there are various parameter to be optimised while printing which are : stand-off distance, overlap distance, laser speed, laser fluence, shutter speed.

There are several deposition parameters to be controlled i.e. stand-off distance, power, deposition time, argon flow rate, substrate heating, chamber pressure.

### **3.2 Characterization techniques:**

The synthesized graphene is studied using various characterization techniques for material confirmation. The morphological characterization is performed using FE-SEM and physical characterization of material is preformed using X-Ray diffraction and Raman mapping.

### 3.2.1 X-Ray Diffraction

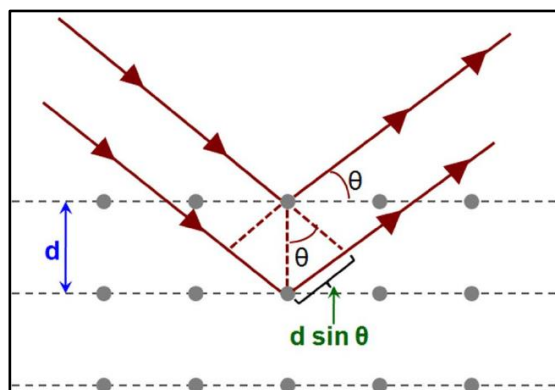


Figure 3.8 Bragg's diffraction law



Figure 3.9 X-ray diffraction unit

X-Ray diffraction technique is a non-destructive often used to identify and analyze the crystal structure, degree of crystallinity and availability of impurity phases if any. it works on the principle that when a high-energy beam falls over a target material, energy absorption happens, and electrons jumps from inner to outer shell thus in an unstable state condition. Due to natural tendency of electrons to reach back to initial stable state, the electrons come back to its original state thus releasing X-rays . The electrons moving from M shell to K shell generates  $K\beta$  x-rays and the ones moving from L shell to K shell generates  $K\alpha$  x-rays. the basic principle of analysis of XRD is based on Bragg's law which states that "When a collimated beam of x-rays strikes

a crystal, the atoms act as diffraction centers and the diffracted beams combine to give diffraction patterns."

**Bragg's Law in a 2-D crystal :** For nth order diffraction, using the X-rays of wavelength  $\lambda$ , the Bragg's equation is:

$$n \lambda = 2d \sin \theta$$

in this work, X-ray diffractometer (Bruker-D2Phaser, with Cu-K radiation) is employed to confirm the crystalline points of graphene synthesized. here XRD patterns are recorded in the range of  $5^\circ$  to  $60^\circ$ .

### **3.2.2 Field Emission Scanning Electron Microscopy (FESEM):**

To study the morphology and its variations over the different energy variations, FE-SEM is used. It is a high-resolution technique where electron beam emitted by field emission source strikes the surface of the sample placed under it. It is then raster scanned to obtain the microstructure and surface morphology at varying magnifications. The inner arrangement of setup is such that the ejected electron beam passes through an arrangement of magnetic lenses and metal apertures in a vacuum tube for focusing as a thin monochromatic beam. when incident electron beam interacts with sample, it generates output beams made up of Auger electrons, secondary electrons, backscattered electrons, and recognisable X-rays with different detectors collecting each type of electron and hence produces images of the sample specimen.



**Figure 3.10 FESEM**

### **Field Emission Scanning electron microscope (FE-SEM)**

Backscattered electrons are produced as a result of the elastic contact between the sample and the electron beam as it exits the source. However, some electrons from the sample are reflected back or backscattered because they do not interact with the nucleus of the specimen. It has been shown that the backscattered electron relies on the element's atomic weight. Higher atomic mass elements produce more backscattered electrons due to greater deflection from larger nuclei. It provides more accurate information about the sample's topography and composition. Secondary electrons are produced by the sample's inelastic interaction with the electron beam. The energy is lower than that of backscattered electrons because of the loss of inelastic contact. To maximise the detector's efficiency, the secondary electron detector is placed at an angle to the incident beam's axis. Secondary electrons are helpful for analysing the surface morphology of a material. This inquiry makes use of a Field- emission scanning electron microscope (FE-SEM, JEOL JSM-7400F) to look at the morphology of sample surfaces that have been coated with gold.

### **3.3 TENG Performance testing setup**

#### **3.3.1 Tribo Testing setup :**

The tribo-setup comprises of :

(a) Potentiometer-controlled arrangement: A potentiometer is attached in the circuitry to manage the variable frequency of tapping. The stepper motor used in the arrangement has capability to move at a maximum voltage of 12 V , current of 2 Amps, step angle of 1.8 degrees and the maximum frequency of tapping that is achieved is 7.5 Hz.

(b) A movable Y axis bed is arranged to adjust the bed height and sample height based on our requirement

(c) Complete setup is controlled with an Arduino and motor driver arrangement.

Figure below shows the sectional view of our tribo-testing machine with all necessary setup arrangements well displayed. A front view display of the setup and side view display is also attached here to get a better understanding of the arrangement.

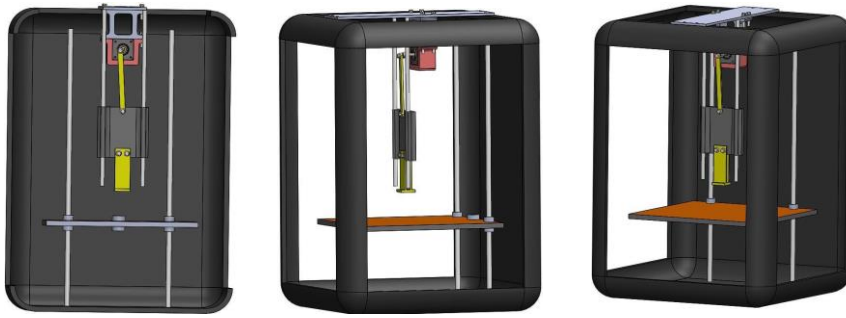


Figure 3.11 Tribo-tapping setup

### 3.3.2 Current and Voltage measuring Setup :



Figure 3.12 oscilloscope and Electrometer

#### Oscilloscope:

Signals in the time and frequency domains can be seen on mixed domain oscilloscopes. They can show synchronised analogue waveforms, digital waveforms, and decoded serial protocols in the time domain. They have an integrated spectrum analyzer signal path with specifications of 121 ps, 150 Mhz frequency, 4 analogue, and 150 Mhz to 1Ghz bandwidth for frequency domain analysis.

#### Electrometer :

The Model 6514 Electrometer offers versatile interface possibilities along with greater resolution, faster speed, charge measuring capabilities, and current sensitivity, with current range upto 1pA , voltage range 2-200 V and charge range 20 nC

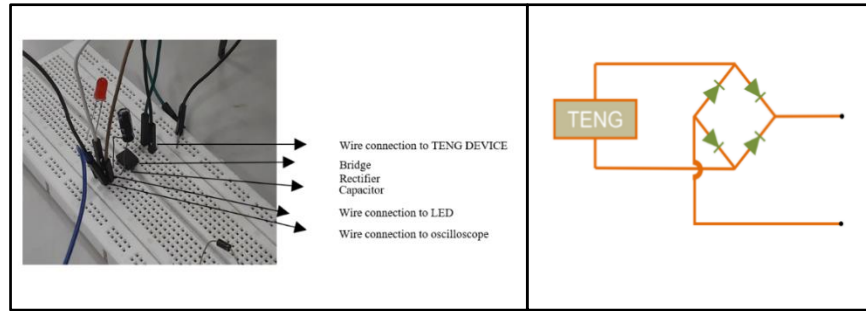


**Figure 3.13 TENG circuit**

Experimental setup encompasses process and device from fabrication stage to output testing stage i.e., from sputtering to characterization to O/P testing.

## Chapter 4

### Parametric investigation for 2D printing of ZnO structure for TENG application

Laser energy is varied based on varying parameter to optimize the printing of ZnO on the ITO coated glass and further nanostructure growth is done on substrate ,after observation is made of the printed structure and hence printing parameter are finalized and later device is fabricated.

#### 4.1 Influence of laser fluence on the track printed ZnO :

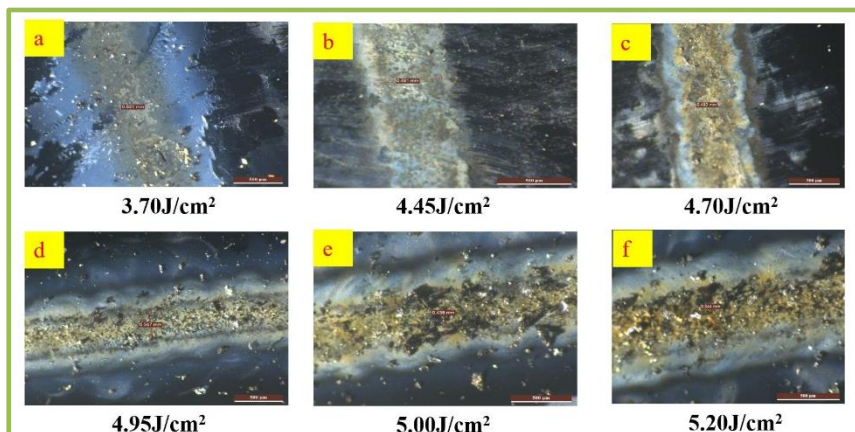


Figure 4.1 Track deposition at varying laser fluences

Initially experiment started with the irradiation of 50 W laser but the applied energy was not sufficient to remove of the material from the silicon wafer and with increase in laser fluence material removal started happening with increase in laser increase there was spattering observed and with less fluence not enough material removal was observed.

With the help of above SEM micrograph laser fluence of  $4.45\text{J}/\text{cm}^2$  was selected as optimized fluence as after that fluence transfer was non uniform.

$$\text{Laser fluence} = \frac{P \times 4}{f \times \pi \times d^2}$$

Where  $v$  denotes scan speed in mm/s,  $d$  is the spot radius in mm,  $f$  is the repetition rate in (1/sec),  $P$  is average laser power (W).

#### 4.2 Influence of spot overlap on the track printed of ZnO:

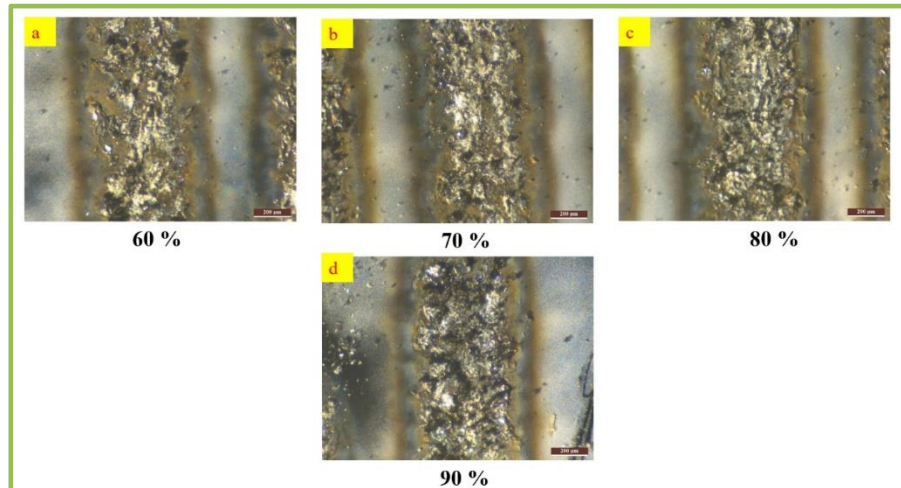


Figure 4.2 Track Deposition at varying overlap percentage

With the help of images taken from the optical microscope at different overlap percentage like 60%,70%,80%,90%. With the help of visual observation, it is seen that, that with increasing spot overlap percentage thickness of the linear track deposited increases. Thus to make trade-off between the thickness and uniformity 80% overlap was selected. And device fabricated on that percentage. And further growth performed.

### 4.3 Influence of growth temperature on the

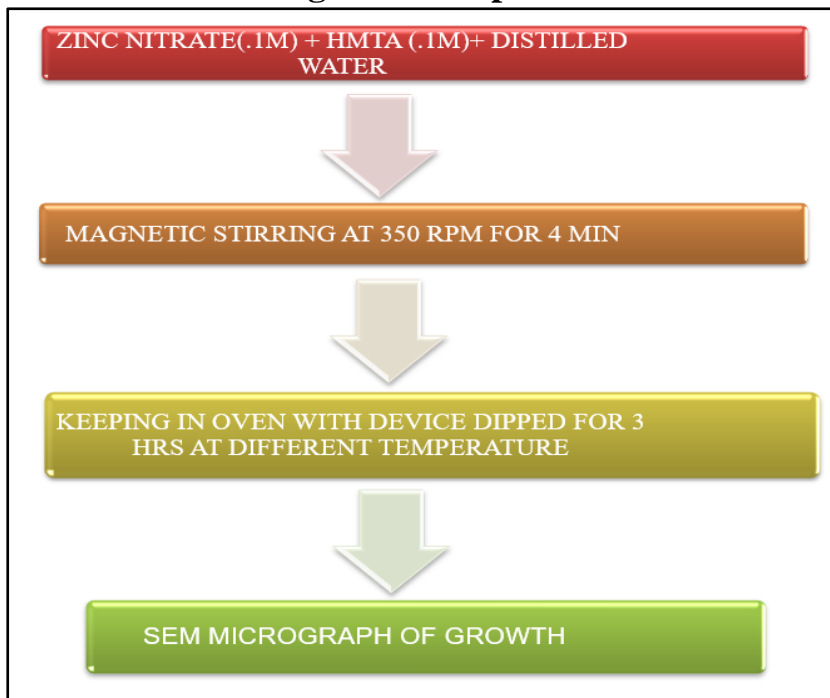


Figure 4.3 Hydrothermal Growth process

### nanostructure ZnO steps:

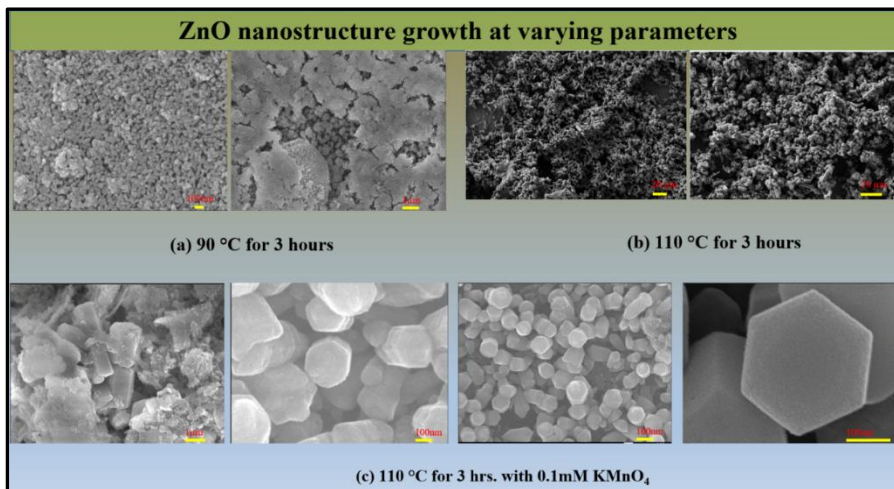


Figure 4.4 SEM micrographs of varying growth

Nanostructure growth means growth of nanorods, nanotubes, dots etc. on the surface here on the transferred pattern with the growth of nanostructure it has been observed that performance betterment is their like: higher charge flow (higher aspect ratio), higher voltage of the device fabricated and hence growth is preferred for good performance.

**Growth At 90° C :** at 90°C (below boiling point of DI water) it was observed that growth of nanoparticle had started but growth is not significant and high amount of precipitate is there and growth is not inclined/ oriented.

**Growth At 110° C :** at 110°C (above boiling point of DI water) it was observed that growth of nanoparticle was there but it was of non-aligned manner like powder form with no or less adhesion to surface.

**Growth At 110° C (with KMnO<sub>4</sub>) :** at 110°C (above boiling point of DI water) with added KMnO<sub>4</sub> it was observed that growth was of aligned nature, big nanorods being formed.

From above study affect of various parameter on Film deposition came into light with increase in laser fluence abrupt of the deposited increased but material transferred increased, with increase in overlap percentage thickness of the track deposited increased and as well abruptness increased and while hydrothermal growth optimised condition was achieved at 110° C with the addition of KMnO<sub>4</sub> where growth of the Nanostructure was aligned and was solid.

## Chapter 5

### TENG Performance Analysis

In the final part of the study, the idea is to use ZnO printed pattern over ITO coated glass as tribo-positive material and FEP sheet coated with copper as tribo-negative material in the triboelectric pair device.

To initially start the experiment, the idea is towards developing an arrangement where samples can be tapped and tested so that it can be used for tribo-testing applications. Tapping with hand will never give uniform results as it will always have error in experiments and hence to solve this issue, a tribo-tapping setup is designed and fabricated for work.

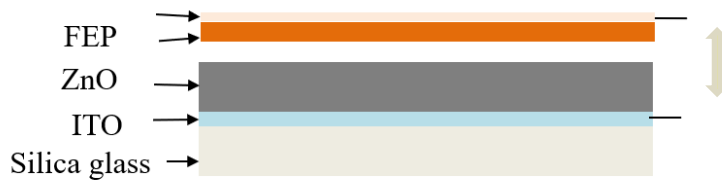


**Figure 5.1 Multilayer schematic for TENG device**

Further the device is connected with oscilloscope and Electrometer to measure the Voltage and current.

After measurement using electrometer and oscilloscope graphs were plotted on voltage vs time graphs and current vs time graphs. And further trends were analysed and difference has to be noted between the grown and non-grown sample, readings are peak current in grown sample increased tenfold, Peak- to-peak voltage difference is observed increasing in grown sample lower noise band has been observed in grown sample. In Peak current graph increasing trend is being observed wrt. RPM and with voltage no Trend were observed.

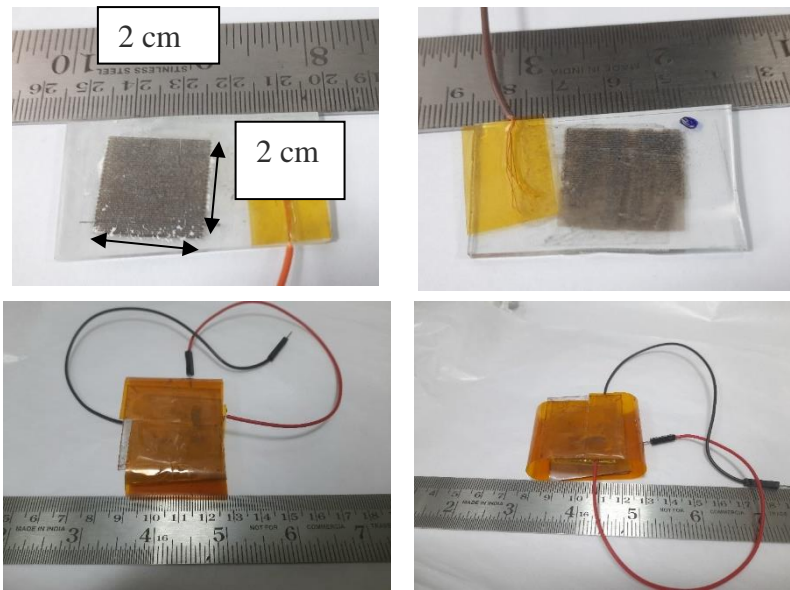


**Figure 5.2 ZnO printed on ITO coated glass with fabricated device**

## 5.1 Current and Voltage vs. Time Characteristics at various Tapping rate Rate:

Voltage vs Time plot at varied RPM(tapping rate)

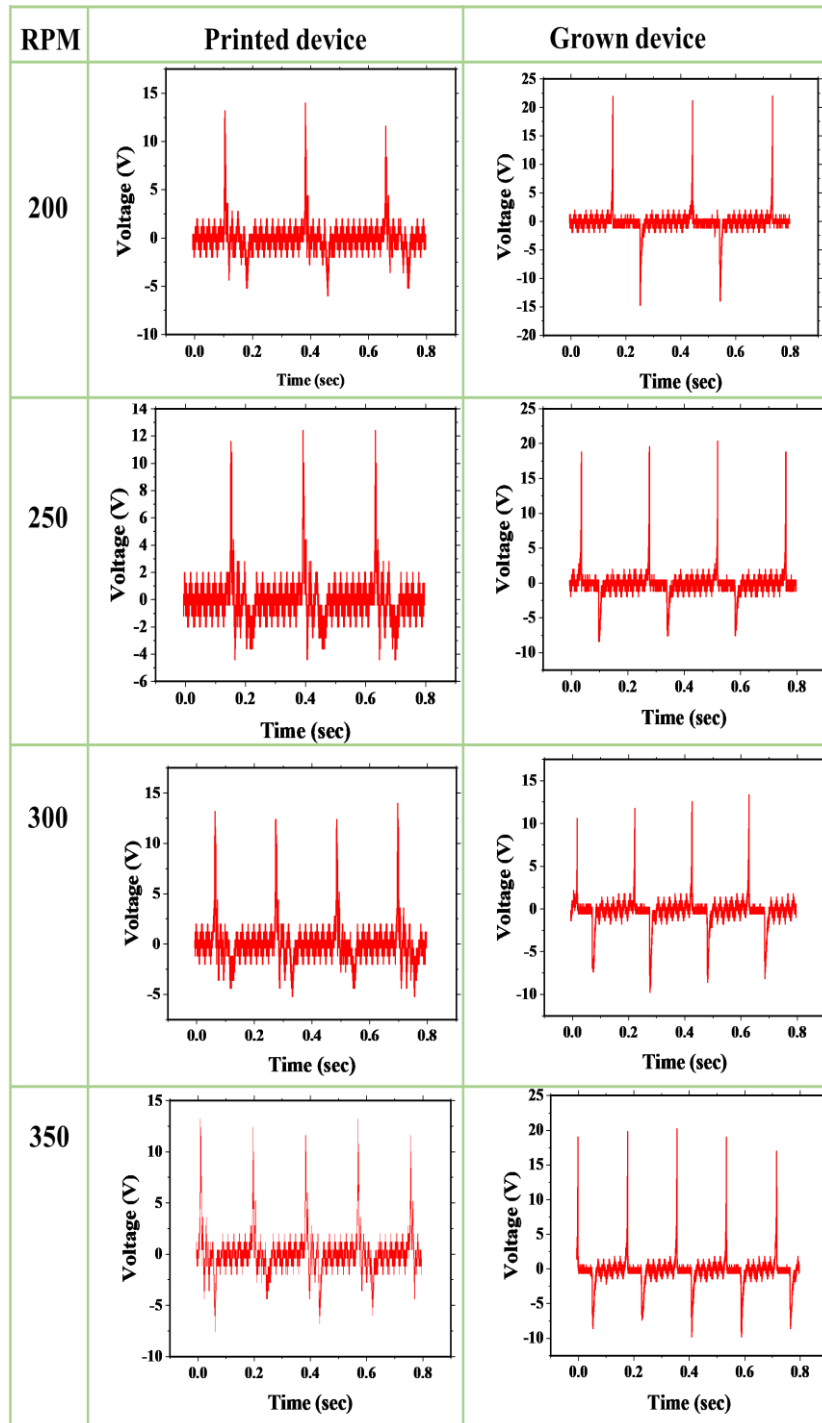


Figure 5.3 Voltage vs. time at varied tapping rate

### Current vs Time plot at varied RPM(tapping rate)

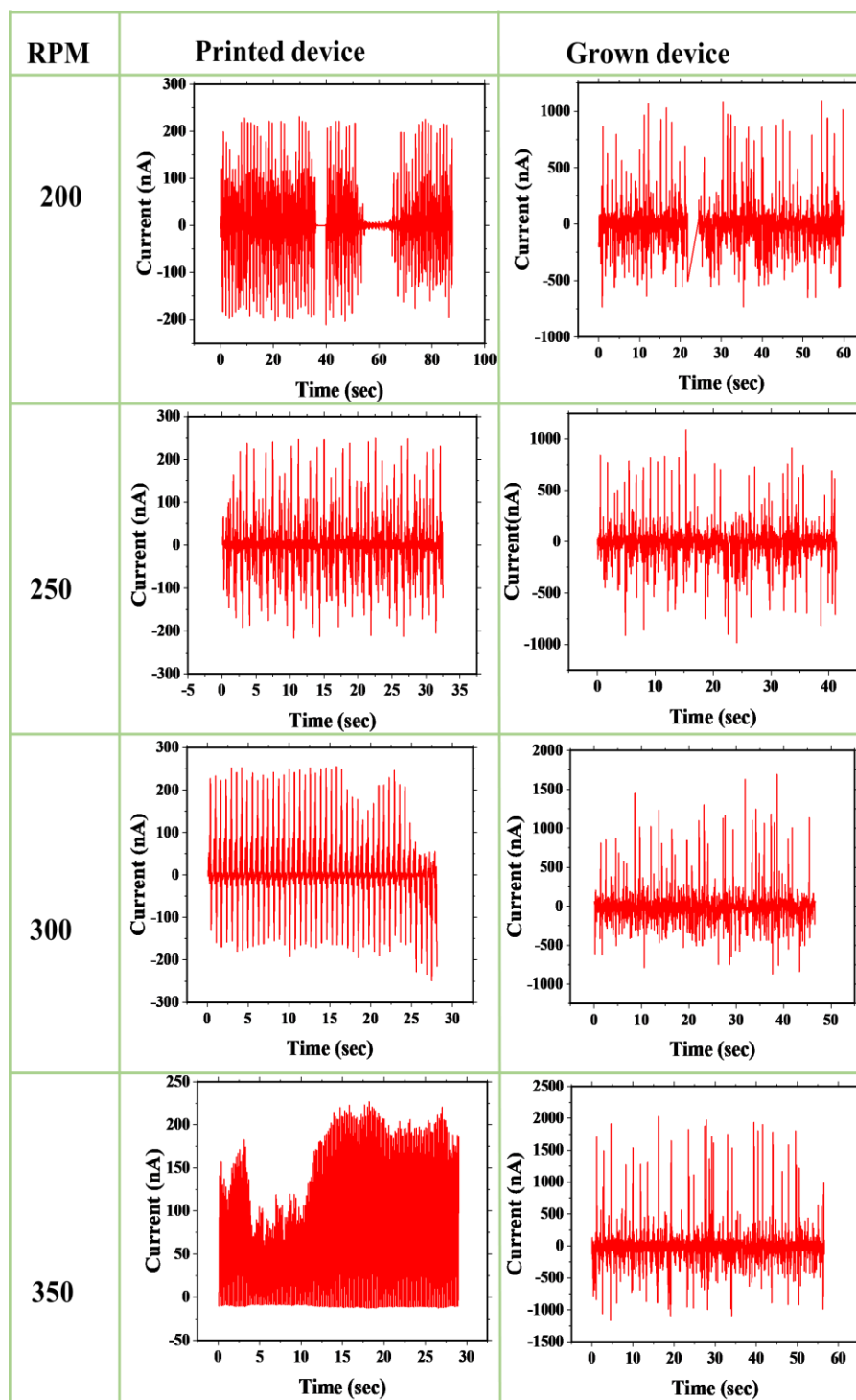


Figure 5.4 Current vs. time at varied tapping rate

## 5.2 Combined voltage vs Tapping rate and Current vs Tapping rate graphs

Current vs RPM is drawn and hence high increase in current with growth is observed and voltage difference also increases with RPM current increase is about tenfold as compared to normal one about 200 nA to 2  $\mu$ A. Peak- to-peak voltage difference is observed increasing in grown sample lower noise band has been observed in grown sample. In Peak current graph increasing trend is being observed wrt. RPM and with voltage no Trend were observed.

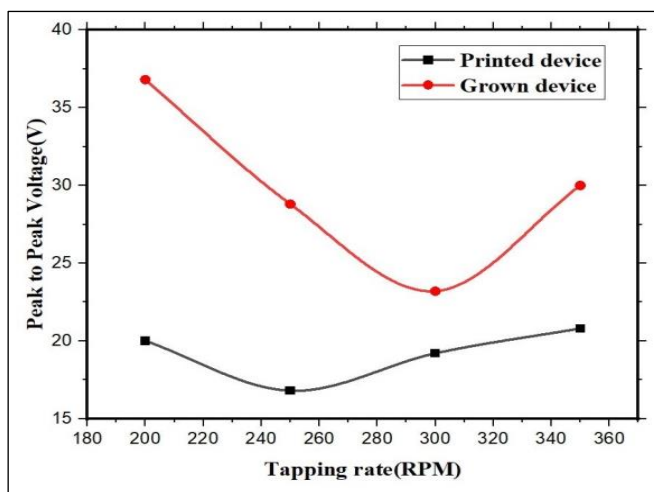


Figure 5.6 Voltage Graph

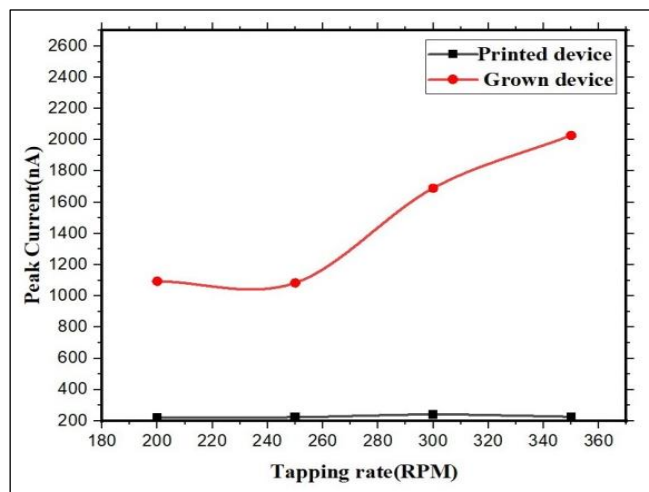


Figure 5.5 Current Graph

### 5.3 XRD plot of ZnO deposited on silicon wafer and ZnO deposited on ITO coated glass

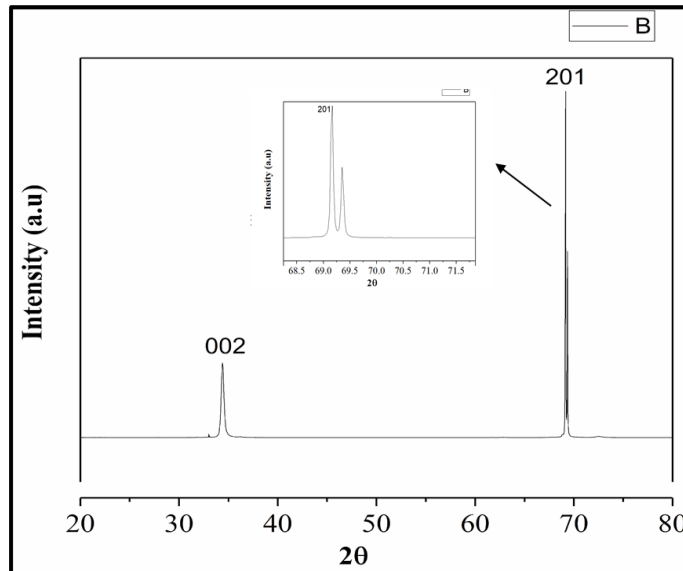


Figure 5.7 XRD plot for ZnO donor

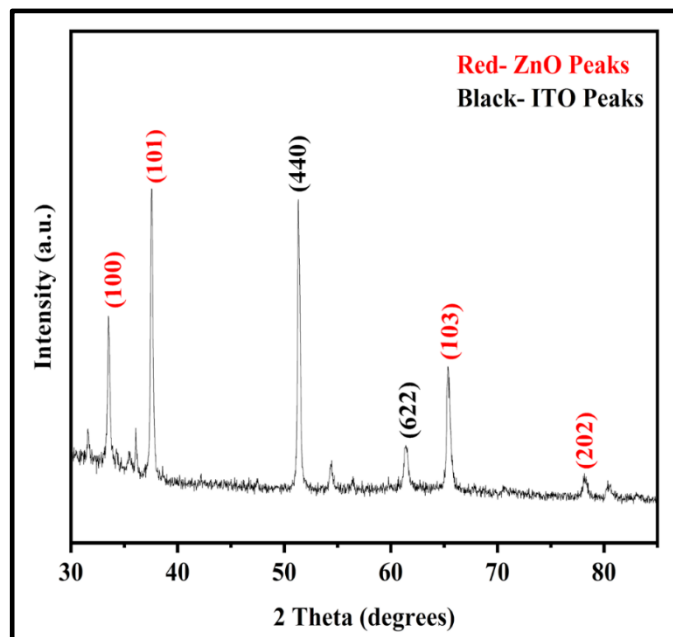


Figure 5.8 XRD plot for ZnO Printed on ITO coated Glass

XRD analysis of the deposited donor substrate was done and ZnO transferred on ITO was also analysed with XRD, thereby several peaks of ZnO was identified with respect to ZnO donor substrate,

From figure 5.7 peak was identified at  $34.39^\circ$  which was of (002) with lattice parameter as  $a=b \neq c$  space group was P -4 3 m other identifies

peak of ZnO was indexed at  $69.16^\circ$  was of (201) with lattice parameter  $a=b\neq c$  with space group as  $Fm\bar{3}m$  peaks of silicon wafer was also observed.

From figure 5.8 ZnO and ITO peaks were identified with respect to printed device In fabricated device, ZnO transferred over ITO peaks were ZnO peaks identified peaks was at various plane

at  $31.29^\circ$  (100) plane peak was identified with lattice parameter  $a=b\neq c$  and  $P63mc$  as space group, at  $37.50^\circ$  peak of (101) was identified with lattice parameter  $a=b\neq c$  and space group as  $P63mc$ , at  $65.8^\circ$  (103) peak was identified with lattice parameter as  $a=b\neq c$  and space group  $P43m$ , at  $78.5^\circ$  (202) peak was identified with lattice parameter as  $a=b\neq c$   $P43m$  and space group

ITO peaks : (440) , (622)

Peaks verified from JCPDS files. With COD Id as 2300450, 1534836, 1536063

#### **5.4 Adhesion characteristics of grown and printed sample with or without substrate heating**

Adhesion analysis performed on the grown vs printed sample with or without substrate heating has been performed where all the above-mentioned process has been used to print/grow the sample and after that heating in oven is performed at  $300^\circ\text{C}$  for 3 hrs. and later with using Image J image processing is done.

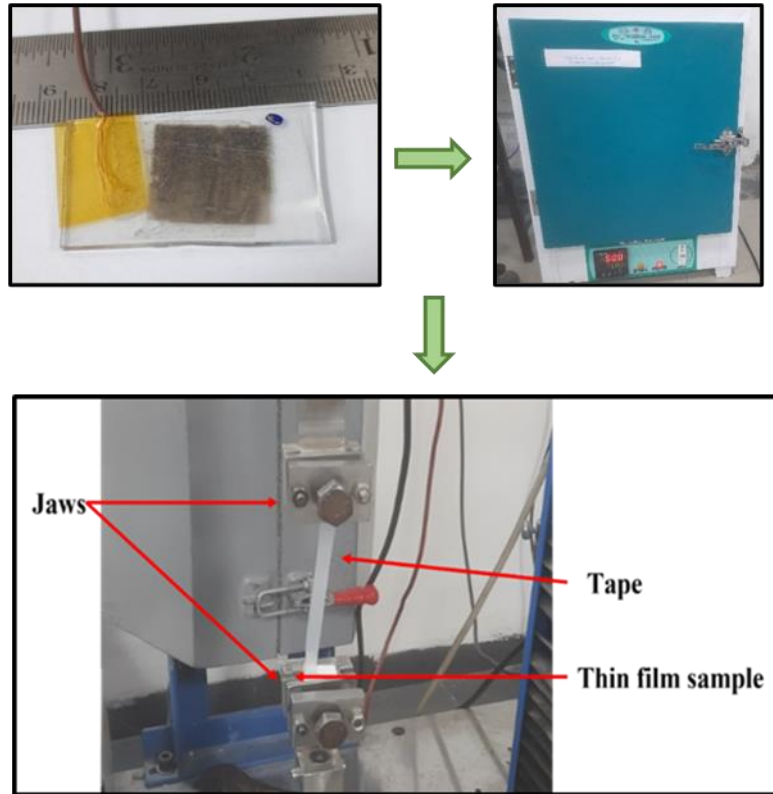


**Figure 5.9 Scotch Tape test**

After whole process optical microscope image of tape is taken and further analysis using Image J is performed i.e.

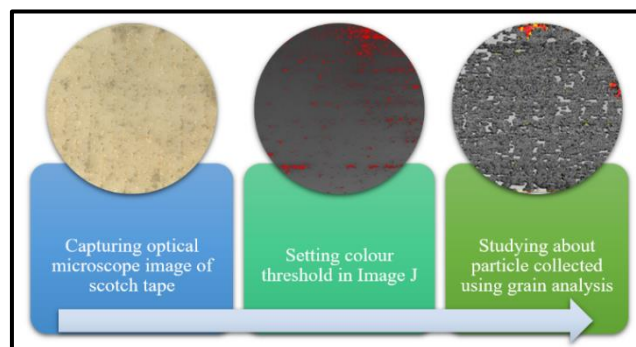


**Figure 5.10 Image J analysis process**

And data calculated after image J analysis is as shown in table below: conclusion from the table given below is that , that with growth mass increases and therefore larger chunks of material removal is observed and with annealing material removal decreases( adhesion improves) and removal of material was uniform. And with performance testing it has

been observed that device with nanoparticle growth performance improved so grown device was selected and with annealing.

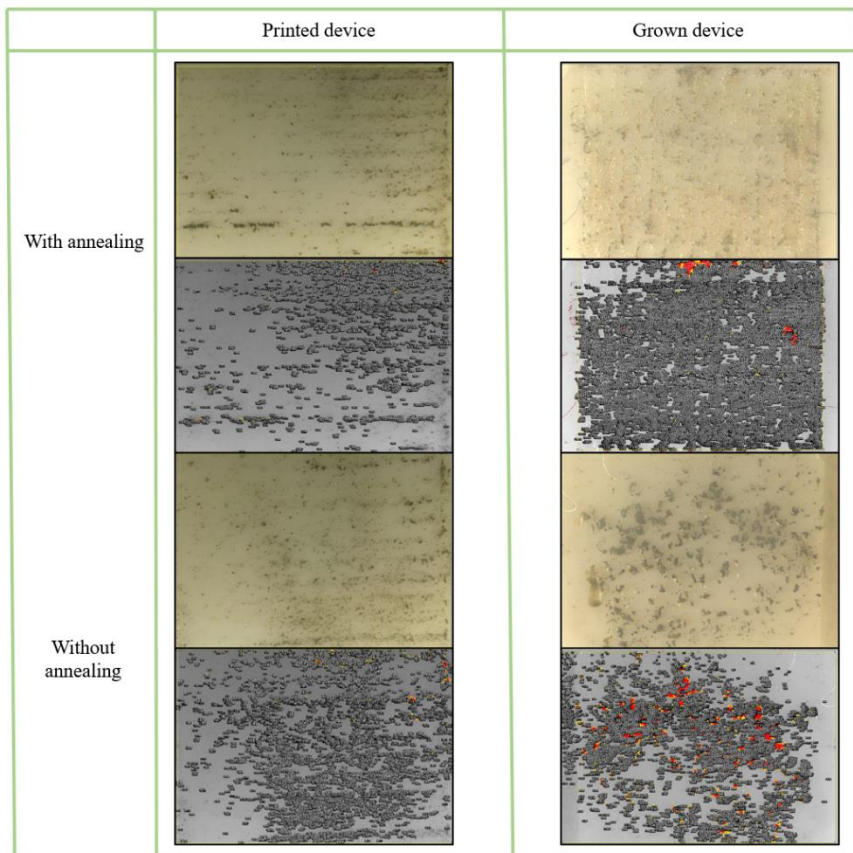


Figure 5.11 grain selection during image analysis

	Without growth	With growth
With Annealing	1.531%	8.204%
Without Annealing	4.034%	9.242%

Table 5.1 Image analysis testing result

From above study it was confirmed that material being transferred is ZnO and device fabricated also contained ZnO which was confirmed by the XRD peaks, Performance testing showed that device having printed with Hydrothermal growth had better Voltage and Current response

Current was even 10 X more than normal Printed and increased with the tapping rate one Voltage just increased by 10 to 15 V.

## Chapter 6

---

### conclusion and Future scope of work

In this overall study, laser has been used to Transfer ZnO (as tribopositive layer) on ITO coated glass and further laser parameter has been modified and optimised to make TENG device, morphological changes have been observed in transferred ZnO with parameter, finally TENG device testing performed.

#### 6.1 Conclusions

- A 10.6  $\mu\text{m}$  CO<sub>2</sub> laser is used for making of ZnO track by irradiating PDMS coated silicon wafer and perform laser induced forward transfer.
- The laser optimization is performed by varying distance between laser and donor substrate, repetition rate and duty cycle and finally ZnO track is transferred.
- The study is further progressed such that effect of pulse overlap at varying laser fluences is considered and a detailed study is performed in that specific direction.
- Based on the study, it is observed that as the pulse overlap increases, there is a increase in material transferred and hence laser pulse overlap on a higher side is studied i.e., 60%, 70%,80%, 90% laser pulse overlap.
- with increase of laser fluence it was observed that material deposition increases but uniformity is compromised
- From XRD analysis, several peaks of ZnO were observed at both at deposited stage and device fabricated stage conforming material presence EDS also confirms material presence.
- Finally transferred ZnO is used as TENG device where ZnO backed with ITO electrode as Tribo-positive layer and FEP backed with copper electrode as Tribo-negative layer and hence making a tribo-pair.

Based on tribo testing using in house made tapper unit voltage generated was almost in the range of 40V and current is in the range of 4  $\mu$ A. The overall study gives a study of a novel method of fabrication and testing of tribo-electric device which doesn't require masking technique for making thin film and is cost effective.

## **6.2 Future scope of work:**

Based on the study parameters, the work can be taken ahead to develop some good amount of tribo energy and can be practically used as a device for real life applications. The future scope of work includes.

(a) Improvement in Tribo-electric Performance: based on the experimental experience, it is observed that with optimised growth parameter, feed rate, shutter frequency, power O/P better surface finish and material uniformity can be achieved.

(b) different laser source: different laser source i.e., other than 10.6  $\mu$ m can be used such that better deposition might be seen

(c) this transfer mechanism of LIFT can be used for fabrication of other new device like piezoelectric devices, doping foreign material into thin film etc.

## References :

- [1] J. Li, N. A. Shepelin, P. C. Sherrell, and A. V. Ellis, “Poly(dimethylsiloxane) for Triboelectricity: From Mechanisms to Practical Strategies,” *Chemistry of Materials*, vol. 33, no. 12. American Chemical Society, pp. 4304–4327, Jun. 22, 2021. doi: 10.1021/acs.chemmater.1c01275.
- [2] J. Lowell and A. C. Rose-Innes, “Contact electrification,” *Adv Phys*, vol. 29, no. 6, pp. 947–1023, Jan. 1980, doi: 10.1080/00018738000101466.
- [3] W. R. Salaneck, A. Paton, and D. T. Clark, “Double mass transfer during polymer-polymer contacts,” *J Appl Phys*, vol. 47, no. 1, pp. 144–147, 1976, doi: 10.1063/1.322306.
- [4] H. T. Baytekin, A. Z. Patashinski, M. Branicki, B. Baytekin, S. Soh, and B. A. Grzybowski, “The Mosaic of Surface Charge in Contact Electrification Downloaded from.” [Online]. Available: <http://science.sciencemag.org/>
- [5] W. G. Kim, D. W. Kim, I. W. Tcho, J. K. Kim, M. S. Kim, and Y. K. Choi, “Triboelectric Nanogenerator: Structure, Mechanism, and Applications,” *ACS Nano*, vol. 15, no. 1. American Chemical Society, pp. 258–287, Jan. 26, 2021. doi: 10.1021/acsnano.0c09803.
- [6] Z. Lin, J. Chen, and J. Yang, “Recent Progress in Triboelectric Nanogenerators as a Renewable and Sustainable Power Source,” *Journal of Nanomaterials*, vol. 2016. Hindawi Limited, 2016. doi: 10.1155/2016/5651613.
- [7] S. Mohan, M. Vellakkat, A. Aravind, and U. Reka, “Hydrothermal synthesis and characterization of Zinc Oxide nanoparticles of various shapes under different reaction conditions,”

Nano Express, vol. 1, no. 3, Dec. 2020, doi: 10.1088/2632-959X/abc813.

[8] C. Te Liu, W. H. Lee, and T. L. Shih, “Synthesis of ZnO nanoparticles to fabricate a mask-free thin-film transistor by inkjet printing,” *J Nanotechnol*, 2012, doi: 10.1155/2012/710908.

[9] X. Huang et al., “Overview of Advanced Micro-Nano Manufacturing Technologies for Triboelectric Nanogenerators,” *Nanoenergy Advances*, vol. 2, no. 4, pp. 316–343, Nov. 2022, doi: 10.3390/nanoenergyadv2040017.

[10] W. Yang et al., “3D stack integrated triboelectric nanogenerator for harvesting vibration energy,” *Adv Funct Mater*, vol. 24, no. 26, pp. 4090–4096, Jul. 2014, doi: 10.1002/adfm.201304211.

[11] Y. Su et al., “Hybrid triboelectric nanogenerator for harvesting water wave energy and as a self-powered distress signal emitter,” *Nano Energy*, vol. 9, pp. 186–195, 2014, doi: 10.1016/j.nanoen.2014.07.006.

[12] K. Y. Lee et al., “Fully Packaged Self-Powered Triboelectric Pressure Sensor Using Hemispheres-Array,” *Adv Energy Mater*, vol. 6, no. 11, Jun. 2016, doi: 10.1002/aenm.201502566.

[13] X. Huang et al., “Overview of Advanced Micro-Nano Manufacturing Technologies for Triboelectric Nanogenerators,” *Nanoenergy Advances*, vol. 2, no. 4, pp. 316–343, Nov. 2022, doi: 10.3390/nanoenergyadv2040017.

[14] B. N. Chandrashekar et al., “Roll-to-Roll Green Transfer of CVD Graphene onto Plastic for a Transparent and Flexible Triboelectric Nanogenerator,” *Advanced Materials*, vol. 27, no. 35, pp. 5210–5216, Sep. 2015, doi: 10.1002/adma.201502560.

[15] S. A. Khan et al., “Flexible Triboelectric Nanogenerator Based on Carbon Nanotubes for Self-Powered Weighing,” *Adv Eng Mater*, vol. 19, no. 3, Mar. 2017, doi: 10.1002/adem.201600710.

- [16] M. Sahu, S. Hajra, J. Bijelic, D. Oh, I. Djerdj, and H. J. Kim, "Triple perovskite-based triboelectric nanogenerator: a facile method of energy harvesting and self-powered information generator," *Mater Today Energy*, vol. 20, Jun. 2021, doi: 10.1016/j.mtener.2021.100639.
- [17] X. Jing et al., "A flexible semitransparent dual-electrode hydrogel based triboelectric nanogenerator with tough interfacial bonding and high energy output," *J Mater Chem C Mater*, vol. 8, no. 17, pp. 5752–5760, May 2020, doi: 10.1039/c9tc06937b.
- [18] W. Xu, L. B. Huang, M. C. Wong, L. Chen, G. Bai, and J. Hao, "Environmentally Friendly Hydrogel-Based Triboelectric Nanogenerators for Versatile Energy Harvesting and Self-Powered Sensors," *Adv Energy Mater*, vol. 7, no. 1, Jan. 2017, doi: 10.1002/aenm.201601529.
- [19] Y. H. Ko, G. Nagaraju, S. H. Lee, and J. S. Yu, "PDMS-based triboelectric and transparent nanogenerators with ZnO nanorod arrays," in *ACS Applied Materials and Interfaces*, American Chemical Society, May 2014, pp. 6631–6637. doi: 10.1021/am5018072.
- [20] H. Zhang et al., "Three-Dimensional Polypyrrole Nanoarrays for Wearable Triboelectric Nanogenerators," *ACS Appl Nano Mater*, 2022, doi: 10.1021/acsanm.2c02357.
- [21] P. Supraja et al., "A simple and low-cost triboelectric nanogenerator based on two dimensional ZnO nanosheets and its application in portable electronics," *Sens Actuators A Phys*, vol. 335, Mar. 2022, doi: 10.1016/j.sna.2022.113368.
- [22] M. Sahu et al., "Development of triboelectric nanogenerator and mechanical energy harvesting using argon ion-implanted kapton, zinc oxide and kapton," *Mater Lett*, vol. 301, Oct. 2021, doi: 10.1016/j.matlet.2021.130290.
- [23] H. H. Singh and N. Khare, "Improved performance of ferroelectric nanocomposite flexible film based triboelectric

nanogenerator by controlling surface morphology, polarizability, and hydrophobicity,” *Energy*, vol. 178, pp. 765–771, Jul. 2019, doi: 10.1016/j.energy.2019.04.150.

[24] A. Sahu, I. A. Palani, and V. Singh, “Investigation on fabrication of NiTi based strain gauge using laser decal transfer based  $\mu$ -3D printing,” *Manuf Lett*, vol. 32, pp. 49–53, Apr. 2022, doi: 10.1016/j.mfglet.2022.03.001.

[25] Yang, W.; Chen, J.; Jing, Q.; Yang, J.; Wen, X.; Su, Y.; Zhu, G.; Bai, P.; Wang, Z.L. 3D Stack Integrated Triboelectric Nanogenerator for Harvesting Vibration Energy. *Adv. Funct. Mater.* 2014, 24, 4090–4096.

[26] Su, Y.; Wen, X.; Zhu, G.; Yang, J.; Chen, J.; Bai, P.; Wu, Z.; Jiang, Y.; Wang, Z.L. Hybrid triboelectric nanogenerator for harvesting water wave energy and as a self-powered distress signal emitter. *Nano Energy* 2014, 9, 186–195.

[27] Lee, K.Y.; Yoon, H.-J.; Jiang, T.; Wen, X.; Seung, W.; Kim, S.-W.; Wang, Z.L. Fully packaged self-powered triboelectric pressure sensor using hemispheres-array. *Adv. Energy Mater.* 2016, 6, 1502566.

[28] Zhang, W.; Diao, D.; Sun, K.; Fan, X.; Wang, P. Study on friction-electrification coupling in sliding-mode triboelectric nanogenerator. *Nano Energy* 2018, 48, 456–463.

[29] Parajuli, P.; Sharma, B.; Behlow, H.; Rao, A.M. Fullerene-Enhanced Triboelectric Nanogenerators. *Adv. Mater. Technol.* 2020, 5, 2000295.

[30] Xu, C.; Liu, Y.; Liu, Y.; Zheng, Y.; Feng, Y.; Wang, B.; Kong, X.; Zhang, X.; Wang, D. New inorganic coating-based triboelectric nanogenerators with anti-wear and self-healing properties for efficient wave energy harvesting. *Appl. Mater. Today* 2020, 20, 100645.